



Published in final edited form as:

J Med Chem. 2015 September 10; 58(17): 6994–7006. doi:10.1021/acs.jmedchem.5b00900.

Design of HIV-1 Protease Inhibitors with Amino-bis-tetrahydrofuran Derivatives as P2-Ligands to Enhance Backbone-Binding Interactions: Synthesis, Biological Evaluation and Protein-ligand X-ray Studies

Arun K. Ghosh^{*,†}, Cuthbert D. Martyr[†], Heather L. Osswald[†], Venkat Reddy Sheri[†], Luke A. Kassekert[†], Shujing Chen[†], Johnson Agniswamy[‡], Yuan-Fang Wang[‡], Hironori Hayashi, Manabu Aoki^{§,^}, Irene T. Weber[‡], and Hiroaki Mitsuya[§]

[†]Department of Chemistry and Department of Medicinal Chemistry, Purdue University, West Lafayette, IN 47907, USA

[‡]Department of Biology, Molecular Basis of Disease, Georgia State University, Atlanta, Georgia 30303, USA

Departments of Infectious Diseases and Hematology, Kumamoto University Graduate School of Biomedical Sciences, Kumamoto 860-8556, Japan

[^]Department of Medical Technology, Kumamoto Health Science University, Kumamoto 861-5598, Japan

[#]Center for Clinical Sciences, National Center for Global Health and Medicine, Tokyo 162-8655, Japan

[§]Experimental Retrovirology Section, HIV and AIDS Malignancy Branch, National Cancer Institute, National Institutes of Health, Bethesda, MD 20892, USA

Abstract

Structure-based design, synthesis, and biological evaluation of a series of very potent HIV-1 protease inhibitors are described. In an effort to improve backbone ligand-binding site interactions, we have incorporated basic-amines at the C4 position of the bis-tetrahydrofuran (bis-THF) ring. We speculated that these substituents would make hydrogen bonding interactions in the flap region of HIV-1 protease. Synthesis of these inhibitors was performed diastereoselectively. A number of inhibitors displayed very potent enzyme inhibitory and antiviral activity. Inhibitors **25f**, **25i**, and **25j** were evaluated against a number of highly-PI-resistant HIV-1 strains and they exhibited improved antiviral activity over darunavir. Two high resolution X-ray structures of **25f** and **25g**-bound HIV-1 protease revealed unique hydrogen bonding interactions with the backbone carbonyl group of Gly48 as well as with the backbone NH of Gly48 in the flap

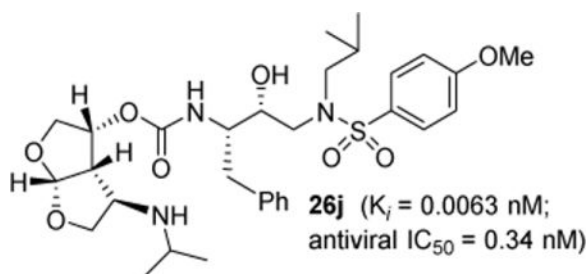
*The corresponding author: Department of Chemistry and Department of Medicinal Chemistry, Purdue University, 560 Oval Drive, West Lafayette, IN 47907, Phone: (765)-494-5323; Fax: (765)-496-1612, akghosh@purdue.edu.

Supporting Information: HPLC and HRMS data of inhibitors **25a–25l**. Crystallographic data collection and refinement statistics for inhibitors **25f** and **25g**-bound HIVP X-ray structures.

The PDB accession codes for **25f** and **25g**-bound HIVP X-ray structures are 5BRY and 5BS4

region of the enzyme active site. These ligand-binding site interactions are possibly responsible for their potent activity.

TOC Image



Keywords

HIV-1 protease inhibitors; Darunavir; amino-bis-THF; multidrug-resistant; design; synthesis; X-ray crystal structure; backbone binding

Introduction

Human immunodeficiency virus type 1 (HIV-1) protease is an essential enzyme critical to viral maturation and infectivity.^{1,2} Therefore, HIV-1 protease is an important drug-design target. The development of protease inhibitors and their introduction into the active antiretroviral therapy led to significant improvement of quality of life, enhanced HIV management, and renewed the mortality and morbidity of HIV/AIDS patients.^{3,4} Despite these improvements, the emergence of drug resistance, high pill burden, and drug side effects are raising serious concerns about the long-term prospects of HIV/AIDS management.^{5,6} The majority of currently approved HIV-1 protease inhibitors contain peptidic-like features which contributed to the poor solubility, oral bioavailability, high serum protein binding, and metabolism by liver microsomes.^{7,8}

The development of new and improved anti-HIV-1 therapeutics, however, is faced with a variety of challenges different from the first and second line therapeutics. These include issues of selection pressure, emergence of multidrug-resistant HIV-1 variants, and cross-resistance.^{9,10,11} Over the years, our research efforts continued to focus on designing nonpeptide protease inhibitors that incorporate stereochemically defined, cyclic ether-derived, novel ligands.^{12,13,14} We reported the design and discovery of many HIV-1 protease inhibitors with intriguing structural features including the development of darunavir (**1**, Figure 1). In darunavir, we incorporated a 3(*R*), 3*a*(*S*), 6*a*(*R*)-bis-tetrahydrofuran (bis-THF) and a hydroxyethylsulfonamide isostere.^{15,16} Darunavir exhibited excellent activity against a wide range of multidrug-resistant HIV-1 variants.^{17,18} Our X-ray structural studies of darunavir-bound HIV-1 protease revealed extensive hydrogen bonding interactions with the active site backbone atoms of HIV-1 protease.¹⁹ One of our major inhibitor design objectives is to promote maximum interactions, particularly hydrogen bonding interactions with backbone atoms. This ‘backbone binding concept’ emerged from the observation that there is minimal distortion of the protease backbone around the

enzyme's active site.^{20,21} The X-ray structure of the darunavir-HIV-1 protease complex showed that both oxygens of the bis-THF ligand formed strong hydrogen bonds with the backbone NH's of Asp29 and Asp30 in the enzyme S2 subsite. Furthermore, the P2 carbonyl formed a strong hydrogen bond with the Gly27 backbone and P2' amine functionality formed a strong hydrogen bond with the Asp30 NH in S2'-subsite. The backbone hydrogen bonds from the S2 to S2'-subsites are conceivably responsible for darunavir's effectiveness against multidrug-resistant HIV-1 variants.^{15, 16}

In an effort to further enhance ligand-binding site interactions, we subsequently incorporated an alkoxy substituent as well as fluorine at the C4 position of bis-THF ligand.^{22,23}

Incorporation of a methoxy substituent at C4 led to inhibitor **3** which showed a water-mediated hydrogen bond with the amide NH of Gly-48 located at the flap of the HIV-1 protease. Also, introduction of *gem*-difluorines at the C4 position resulted in inhibitor **4** which exhibited strong non-bonded interactions with the carbonyl group of Gly48 through the *gem*-difluorides in the flap region of HIV-1 protease. These interactions appeared to be responsible for improved inhibitor affinity, antiviral activity against multidrug-resistant HIV-1 variants, and ability to cross the blood-brain-barrier.^{23,24} In the current studies, we plan to maintain all the key backbone hydrogen bonding interactions through the bis-THF oxygens. In addition, based upon the X-ray structure of **3**-bound HIV-1 protease, we speculated that introduction of secondary amine functionality at the C4 position, as in inhibitor **25j**, may lead to strong hydrogen bonding interactions with the Gly48 backbone atoms. Also, the alkyl side chain may fill in the hydrophobic pocket effectively in the S2 subsite. Overall, this improvement in backbone interactions and van der Waals interactions may not only result in improvement of antiviral activity against multidrug-resistant HIV-1 variants, but the basic amine may also improve the inhibitor's pharmacological properties. Herein we report our enantioselective synthesis of C4-amine-derived bis-THF ligands using a 2,3-sigmatropic rearrangement as the key reaction. We incorporated these ligands into HIV-1 protease inhibitors and evaluated their biological properties. We also carried out X-ray structural studies of inhibitor-HIV-1 protease complexes to gain molecular insight into the ligand-binding site interactions.

Synthesis

Synthesis of the optically active C-4 azide derivative is shown in Scheme 1. The α,β -unsaturated isopropylidene derivative **5** was synthesized from commercially available D-mannitol as described by us previously.²² Dibal-H reduction of ester **5** provided an allylic alcohol which was reacted with *tert*-butylbromoacetate in the presence of cesium hydroxide in CH₃CN at 23° C for 6 h to provide *O*-alkylation product **6** in 88% yield over two steps.^{25,26} Reaction of **6** with LiHMDS in THF at -40 °C to -30 °C for 1 h resulted in a sigmatropic rearrangement, providing α -hydroxy ester **7** as the major product in 62% yield.^{27,28}

The α -hydroxy ester **7** was protected as the benzyl ether **8** in near quantitative yield. It was converted to bis-THF derivative in a three-step sequence involving, (1) reduction of **8** by LiAlH₄ in THF at 0 °C to 23 °C to provide an alcohol; (2) ozonolytic cleavage of the olefin to form an aldehyde, and (3) reaction of the resulting crude aldehyde with *p*-TsOH in

CH₂Cl₂ at 23 °C to provide bis-THF alcohol **9** in 42% yield over three steps. Alcohol **9** was converted to azide **10** under Mitsunobu conditions²⁹ using diphenyl phosphorazidate (DPPA), triphenyl phosphine and diethyl azodicarboxylate (DEAD) at 0 °C to 23 °C for 18 h to provide azide **10** in 73% yield. Removal of the benzyl ether using BBr₃ in the presence of K₂CO₃ at -78 °C to -20 °C for 2 h provided azidoalcohol **11** in 64% yield.³⁰

Azide **10** was then converted to a number of amine derivatives as shown in Scheme 2. Catalytic hydrogenation of **10** over 10% Pd/C in the presence of di-*tert*-butyl dicarbonate (Boc₂O) under a hydrogen filled balloon afforded Boc-derivative **12** in 98% yield. These reaction conditions did not remove benzyl ether. Reduction of azide **10** with Ph₃P in aqueous THF at 23 °C for 24 h provided the corresponding amine. Addition of methyl chloroformate in the presence of saturated aqueous NaHCO₃ solution afforded methyl carbamate **13** in 71% yield. For the synthesis of various *N*-alkylated derivatives, Boc-derivative **12** was treated with NaH in THF at 0 °C for 30 min, and then MeI was added. The resulting mixture was warmed to 23 °C to provide *N*-methyl derivative **14** in 98% isolated yield. For the synthesis of *N*-ethyl derivative, Boc-derivative **12** was reacted with cesium hydroxide and ethyl iodide in DMF at 60 °C to provide the *N*-ethyl derivative **15** in 91% yield. Isopropyl derivative **16** was synthesized from azide **10** in a three step process involving reduction of the azide to the amine under hydrogenation conditions, reductive amination with acetone and sodium borohydride to afford the isopropyl amine, and finally Boc protection of the resulting amine with Boc anhydride.

Various ligand alcohols were prepared by deprotection of benzyl ethers. As shown in Scheme 3, amine derivatives **12–16** were subjected to a catalytic amount of Pd(OH)₂ in methanol under a hydrogen-filled balloon to provide alcohols **17–21** in good to excellent yields.

Various optically active ligand alcohols were converted to the corresponding activated mixed carbonates. As depicted in Scheme 4, treatment of ligand-alcohols (**11**, **17–21**) with 4-nitrophenyl chloroformate and pyridine in CH₂Cl₂ at 0 °C to 23 °C for 12 h provided carbonates **22a–f** in very good yields (71–91%). The syntheses of various inhibitors containing hydroxyethylaminesulfonamide isosteres with 4-methoxysulfonamide (**23**) and 4-aminosulfonamide (**24**) as P₂'-ligands are shown in Scheme 5. Reaction of amine **23** with activated carbonate **22a** provided inhibitor **25a** in good yield. Similarly, reaction of carbonates **22b–f** and amine **23** provided inhibitors **25c–e**, **25h**. Inhibitor **25g** was prepared by reaction of amine **24** and carbonate **22b** followed by removal of the Boc group by treatment with TFA in CH₂Cl₂. Catalytic hydrogenation of the azide functionality in **25a** over 10% Pd/C in ethyl acetate provided inhibitor **25b** in excellent yield.

Inhibitor **25f** was prepared by removal of the Boc-group from inhibitor **25d** by treatment with TFA in CH₂Cl₂ at 23 °C for 2 h. Similarly, inhibitor **25i** and **25j** were prepared by removal of the Boc group by treatment with TFA in CH₂Cl₂ at 23 °C for 2–4 h. Inhibitors **25k** and **25l** containing dimethyl and diethyl amine functionalities were prepared by reductive amination of amine **25b** with paraformaldehyde and acetaldehyde respectively to provide **25k** and **25l** (50–53% yield).

Results and Discussions

All inhibitors were evaluated in an HIV-1 protease inhibitory assay according to the protocol described by Toth and Marshall.³¹ Compounds that exhibited potent K_i values, were then selected for further evaluation in an antiviral assay in MT-2 human T-lymphocytes exposed to HIV-1_{LAI}.¹⁷ Inhibitor structures and biological results are shown in Table 1. As can be seen, C-4 substituted amino-bis-THF ligand-derived inhibitors exhibited very potent enzyme inhibitory and antiviral activity. The azide containing inhibitor **25a** displayed very good enzymatic and antiviral activity (entry 1). The corresponding amine-derived inhibitor **25b** showed significant reduction in potency. The Boc-amine derivative **25c**, however, gained substantial potency over the amine derivative **25b** (entries 2 and 3). The corresponding methyl carbamate **25d** has shown comparable activity to Boc-derivative **25c**. *N*-methylation of the Boc-derivative provided inhibitor **25e** with nearly 10-fold loss in antiviral activity, indicating that the NH group may be important for potency (entries 3 and 5). Inhibitor **25f** with a methylamine functionality at C4 turned out to be a potent inhibitor ($K_i = 1.5$ pM and antiviral IC_{50} 35 nM). The corresponding 4-amino sulfonamide derivative **25g**, however, displayed reduction of enzyme inhibitory and antiviral activity (entry 7). We have examined the effect of steric bulk on the amine functionality. The Boc-ethyl derivative **25h** showed comparable enzyme inhibitory activity to the methyl derivative **25e** (entries 5 and 8). The ethylamine derivative **25i** showed slightly improved antiviral IC_{50} value (22 nM) over the methyl derivative **25f** (IC_{50} value 35 nM, entries 6 and 9). A sterically demanding isopropyl amine derivative **25j** showed over 60-fold improvement in antiviral activity over the methyl and ethyl derivatives (entries 6 and 9). The dimethyl amine derivative **25k** and diethylamine derivative **25l** were significantly more potent than the corresponding methylamine and ethylamine derivatives **25f** and **25i** respectively. This result indicates that the dialkylamine is most likely involved in enhanced van der Waals interactions in the S2 subsite of HIV-1 protease. It appears that the C4-position of the bis-THF can accommodate a basic amine functionality with further improvement in antiviral activity compared to unsubstituted bis-THF derivatives.

Inhibitors **25f**, **25i**, and **25j** with basic amine functionalities on the bis-THF ring showed potent antiviral activity. We speculated that the improvement of antiviral IC_{50} is possibly due to additional hydrogen bonding interactions as well as increased lipophilicity of the inhibitors due to improved van der Waals interactions in active site. We selected these inhibitors for further evaluation against highly darunavir-resistant and multi-PI-resistant HIV-1 variants, HIV-1_{DRV}^R_{P10}, HIV-1_{DRV}^R_{P20} and HIV-1_{DRV}^R_{P51}. Antiviral assays using human MT-4 cells exposed to these PI-resistant variants showed that all three inhibitors displayed comparable EC_{50} values ranging from 21 nM to 39 nM against HIV-1_{DRV}^R_{P10} and HIV-1_{DRV}^R_{P20}. Fold changes for inhibitors **25f** and **25i** were very low (1 to 2.6) against HIV-1_{DRV}^R_{P10} and HIV-1_{DRV}^R_{P20}. While inhibitor **25j** showed potent antiviral EC_{50} against HIV-1_{NL4-3}, its fold-changes against these strains were significantly higher (21 to 75-fold). Interestingly, sterically less demanding methyl amine derivative **25f** was equipotent against HIV_{WT} ($EC_{50} = 0.029$ μ M) and HIV-1_{DEV}^R_{P20} ($EC_{50} = 0.032$ μ M), however, inhibitor **25j** with isopropylamine displayed nearly 23-fold poorer in antiviral potency against HIV-1_{DRV}^R_{P20} ($EC_{50} = 0.024$ μ M) compared to that against the wild-type

HIV_{NL4-3} (EC₅₀ = 0.001 μM). Darunavir in the same assay exhibited EC₅₀ value of 0.097 μM against HIV-1_{DRV}^R_{P20}. Both inhibitors **25i** and **25j** showed comparable EC₅₀ value against highly PI-resistant strain HIV-1_{DRV}^R_{P51} and fold changes were 15-fold and 260-fold respectively, indicating higher fold changes with bulkier amine substituent (isopropyl vs. methyl). The fold changes for darunavir was significantly greater. Inhibitors **25i** and **25j** showed 10-fold improvement in EC₅₀ values over darunavir. It turned out that inhibitor **25i** with a smaller ethylamine at C4 position of bis-THF has a greater genetic barrier than inhibitor **25j** with an isopropyl amine at C4. Furthermore, it appears that incorporation of basic amine at C4 leads to inhibitors with greater genetic barrier than unsubstituted inhibitor, such as darunavir. The overall improvement of antiviral activity of amine-derived inhibitors is possibly due to their enhanced backbone interactions as well as van der Waals interactions in the S2 subsite.

To obtain molecular insight into the inhibitor-HIV-1 protease interactions, we have determined the X-ray structures of the methylamine derivative **25f** and HIV-1 protease complex as well as inhibitor **25g** and HIV-1 complex. The structures were refined at 1.34 Å and 1.29 Å resolution, respectively. The crystal structures contain the protease dimer and the inhibitors are seen in two orientations related by a 180° rotation with 60/40% relative occupancies. The overall structures are comparable to the structure of HIV-1 protease with darunavir,³² showing root mean square differences of 0.16 Å and 0.13 Å for Cα atoms, respectively, for the two structures. Differences between equivalent Cα atoms are less than 0.5 Å. The 2Fo-Fc and omit Fo-Fc maps are shown for the inhibitors in both X-ray structures (please see supporting information). The 2Fo-Fc map is contoured at a level of 1.0 σ and the omit map is contoured at 2.0 σ. The two inhibitors differ in the substituents of the phenyl ring at P2', where inhibitor **25f** has a methoxy group and inhibitor **25g** has an amino group. Both inhibitors maintained all the key interactions observed in darunavir bound HIV-1. In addition, the C4-NH was shown to form a unique hydrogen bond with the carbonyl of Gly48 shown in Figure 2 for inhibitor **25f**. This interaction was absent for the oxymethyl oxygen of the related inhibitor, **3** (pdb code: 3QAA).²² The C4-NH also formed a water-mediated hydrogen bonding interactions to amide NH of Gly48. Similar inhibitor and enzyme backbone interactions along with increased van der Waals interactions due to isopropyl group may have significantly contributed towards the increased antiviral activity of inhibitor **25j**. Of particular note, inhibitor **25j** incorporates a basic amine functionality which may improve pharmacological properties of this class of inhibitors.

There are several major types of antiretroviral drugs for treating HIV/AIDS. These drugs interfere with different steps in HIV replication. While the use of antiretroviral therapy (ART) treatment and guidelines are updated constantly with the availability of new drugs, PIs continue to be an important element of current ART. Integrase and reverse transcriptase inhibitors are also widely used in ART regimens. The ART regimens are usually well tolerated, however each drug can have serious side effects. Unlike PIs, one major advantage of integrase inhibitors is that they do not require boosting. However, serious side effects including hepatotoxicity, GI disorders, skin disorders, thrombocytopenia, and renal failure are known to occur.³³ Depending upon situation, in such a scenario, HIV/AIDS patients have to switch to other key drugs, such as PIs. Also, certain patients receiving long-term

ART regimens containing integrase inhibitors tend to harbor HIV-1 variants resistant to integrase inhibitors. Furthermore, patients with heavily-ART regimens-experience tend to have drug-failure with various PIs even with DRV. Thus, more potent PIs with a “high genetic barrier” are critical to effective long-term treatment of HIV/AIDS.

It has been documented that darunavir potently inhibits the replication of not only wild-type HIV-1 but also multidrug-resistant HIV-1 variants. However, the emergence of DRV-resistant HIV-1 variants has been reported *in vitro* and *in vivo* and patients harboring such DRV-resistant HIV-1 variants have had treatment failure.^{34,35} Regarding the emergence of DRV-resistant HIV-1 variants, all three C-4 amino derivatives appeared to be more potent against the DRV-resistant HIV-1 variants. For example, the fold difference in the IC₅₀ value of **25f** against HIV-1_{DRV^RP20} compared to the IC₅₀ value of **25f** against the wild-type HIV-1_{NL4-3} was only 1.1, while the fold difference in the case of DRV was as much as 37.3. Moreover, the fold-differences in the case of **25i** and **25j** with HIV-1_{DRV^RP51} were 15 and 260, respectively, while that in the case of DRV with HIV-1_{DRV^RP51} was as much as 1,346. These data signify that the three C4-modified compounds remain highly active against the DRV-resistant HIV-1 variants. The ligand-binding site interactions of the substituted derivatives are different in the S2-subsite. As shown in Figure 2, the C4-NH of inhibitor **25f** forms a unique hydrogen bond with the carbonyl of Gly48. The C4-NH also forms water-mediated hydrogen bonding interactions to amide NH of Gly48. These interactions, which were absent in the case of DRV,¹⁷ may explain why these inhibitors **25f**, **25i**, and **25j** remain active against the DRV-resistant HIV-1 variants (*e.g.*, HIV-1_{DRV^RP20} and HIV-1_{DRV^RP51}; Table 2).

Of particular note, cleavage site mutations within the retroviral polyprotein, the substrate for HIV-1 protease, are known to play critical roles in HIV-1's acquisition of resistance to various protease inhibitors.³⁶ In this regard, when we successfully selected DRV-resistant HIV-1 variants (*e.g.*, HIV-1_{DRV^RP20} and HIV-1_{DRV^RP51}) using the mixture of 8 multi-drug resistant HIV-1 variants as a starting viral population,³⁵ no additional cleavage site mutations within the polyprotein were identified.³⁵ Instead, H219Q and I223V substitutions, located in the CypA binding loop of the Gag protein emerged in early selection stages. Plus, a unique combination of V32I, L33F, I54M, and I84V substitutions, which appeared to be responsible for the loss of DRV's protease dimerization inhibition activity,^{37,38} was identified within. Although, how these amino acid substitutions contribute to HIV-1's acquisition of resistance to DRV remains to be further elucidated, the C4-modification in the *bis*-THF moiety of DRV may shed light in the better understanding of the mechanism of DRV resistance and further design of more potent and resistance-repellant protease inhibitors.

Conclusion

We have designed and synthesized a series of HIV-1 protease inhibitors containing various C4-amine derivatives. One of objectives of these studies was to incorporate basic amine functionalities that can form hydrogen bonding interactions with the backbone atoms in the flap region of the HIV-1 protease. We have investigated a range of amine functionalities. The synthesis of the corresponding amine-*bis*-THF ligands was carried out stereoselectively

and in an optically active manner. The synthesis involved isopropylidene-D-glyceraldehyde as the optically active starting material and a 2,3-sigmatropic rearrangement as the key reaction which installed two chiral centers with high diastereoselectivity. In general, mono- or disubstituted amine-derivatives on the bis-THF ligand showed excellent enzyme inhibitory and antiviral activity. Inhibitor **25j** with a C4-isopropylamine functionality exhibited the best results. It showed marked antiviral activity with an IC₅₀ value of 0.34 nM, showing over 10-fold improvement compared to darunavir. Inhibitors **25f**, **25i**, and **25j** were evaluated against a panel of multidrug-resistant HIV-1 variants and these inhibitors showed improved antiviral activity over darunavir. We have obtained high resolution X-ray crystal structures of related inhibitors **25f** and **25g** bound to HIV-1 protease. These structures revealed that the C4-NH formed a direct backbone hydrogen bonding interaction with Gly48 carbonyl in the S2-subsite. Furthermore, the C4-NH formed water-mediated hydrogen bonds with Gly48 backbone NH. The improved antiviral activity of **25j** against multidrug-resistant HIV-1 variants is possibly due to similar backbone hydrogen bonding interactions as well as hydrophobic interaction due to the isopropyl group. The basic amine functionality on the inhibitor may improve pharmacological properties. Further studies aimed at optimization of ligand-binding site interactions and improving drug-like properties of these inhibitors are currently in progress.

Experimental Section

General

All anhydrous solvents were obtained according to the following procedures: diethyl ether and tetrahydrofuran (THF) were distilled from sodium/benzophenone under argon; dichloromethane from calcium hydride. All other solvents were reagent grade. All moisture sensitive reactions were carried out in a flame-dried flask under argon atmosphere. Column chromatography was performed with Whatman 240–400 mesh silica gel under low pressure of 3–5 psi. Thin layer chromatography was carried out with E. Merck silica gel 60-F-254 plates. Yields refer to chromatographically and spectroscopically pure compounds. ¹H NMR and ¹³C NMR spectra were recorded on a Varian Inova-300 (300 MHz and 75 MHz, respectively), Bruker Avance ARX-400 (400 MHz and 100 MHz), and Bruker Avance DRX-500 (500 MHz and 125 MHz). High and low resolution mass spectra were carried out by the Mass Spectroscopy Center at Purdue University. The purity of all test compounds was determined by HRMS and HPLC analysis. All test compounds showed 95% purity.

(2Z)-*t*-Butyl 2-((3-((4S)-2,2-dimethyl-1,3-dioxolan-4-yl))allyloxy)acetate (**6**)

Diisobutyl aluminum hydride (1 M in CH₂Cl₂, 27.5 mL, 27.5 mmol) was slowly added to a cold solution (–78 °C) of ethyl (2Z)-3-[(4S)-2,2-dimethyl-1,3-dioxolan-4-yl]-2-propenoate (**5**), (5.5 g, 27.5 mmol) in dichloromethane (100.0 mL). The solution was allowed to stir for 15 min at –78 °C (a color change from colorless to yellow and back to colorless indicates that the reaction is complete). A saturated solution of sodium potassium tartrate (20 mL) was added and the reaction mixture was warmed to room temperature. The reaction was stirred until both layers were transparent. The organic layer was separated and the aqueous layer was extracted with dichloromethane (3 × 15 mL). The organic layers were combined, washed with brine and dried over MgSO₄. The solid was filtered out and the organic layer

was concentrated under vacuum to obtain the desired allyl alcohol. The crude mixture was taken to the next step without purification. $R_f = 0.27$ (40% ethyl acetate/hexanes). $^1\text{H NMR}$ (400 MHz, CDCl_3) δ 5.84–5.81 (m, 1H), 5.55 (t, $J = 8.5$ Hz, 1H), 4.85 (q, $J = 9.6$ Hz, 1H), 4.28 (dd, $J = 6.8, 7.3$ Hz, 1H), 4.18 (d, $J = 4.8$ Hz, 1H), 4.08 (t, $J = 6.5$ Hz, 1H), 3.56 (t, $J = 9.0$ Hz, 1H), 2.12 (bs, 1H), 1.41 (s, 3H), 1.38 (s, 3H). $^{13}\text{C NMR}$ (100 MHz, CDCl_3) δ 133.1, 129.4, 109.4, 71.8, 69.4, 58.5, 26.6, 25.8.

To a round bottom flask containing flame dried 4Å molecular sieves (6.0 g) and acetonitrile (200 mL) was added a solution of (2Z)-3-((4S)-2,2-Dimethyl-1,3-dioxolan-4-yl)prop-2-en-1-ol (27.5 mmol) in acetonitrile (20.0 mL), followed by *t*-butylbromoacetate (4.9 mL, 33.0 mmol), tetrabutylammonium iodide (1.0 g, 2.75 mmol) and cesium hydroxide monohydrate (6.90 g, 41.3 mmol) at room temperature. The reaction was allowed to stir for 6 h. The solid was filtered out and the solvent was concentrated under vacuum; the residue was purified by flash column chromatography (5% ethyl acetate/hexanes) to afford **6** (6.60 g, 88% yield, 2 steps) as a colorless oil. $R_f = 0.57$ (30% ethyl acetate/hexanes). $^1\text{H NMR}$ (400 MHz, CDCl_3) δ 5.78–5.74 (m, 1H), 5.61 – 5.66 (m, 1H), 4.83 (q, $J = 7.4$ Hz, 1H), 4.16–4.20 (m, 2H), 4.09 (dd, $J = 6.2, 2.0$ Hz, 1H), 3.94 (d, $J = 3.1$ Hz, 2H), 3.54 (t, $J = 8.1$ Hz, 1H), 1.47 (s, 9H), 1.34 (s, 3H), 1.31 (s, 3H). $^{13}\text{C NMR}$ (100 MHz, CDCl_3) δ 169.3, 131.4, 129.5, 109.3, 81.6, 71.9, 69.4, 67.7, 66.5, 28.0, 26.6, 25.8. LRMS-ESI (m/z) 273 (M+H).

(2R,3R)-*t*-Butyl 3-(((4S)-2,2-dimethyl-1,3-dioxolan-4-yl))-2-hydroxypent-4-enoate (7)

A solution of LiHMDS (36.0 mL 1 M in THF, 36.0 mmol) was added to a cold solution (-45 °C) of **6** (6.60 g, 24.2 mmol) in THF (100 mL). LiHMDS was added at a rate that did not exceed -40 °C. The reaction mixture was allowed to warm slowly to -30 °C over 1 h. The reaction was quenched with saturated ammonium chloride (20 mL) and extracted with ethyl acetate (3×20 mL) after warming to room temperature. The organic layers were combined, washed with brine, dried over anhydrous MgSO_4 and concentrated under vacuum. The residue was purified with a 5 – 10 percent gradient of ethyl acetate/hexanes. The desired rearranged product **7** (4.10 g, 62% yield) was obtained as a colorless oil. $R_f = 0.49$ (30% ethyl acetate/hexanes). ($^1\text{H NMR}$ (400 MHz, CDCl_3) δ 5.88–5.79 (m, 1H), 5.20 (dd, $J = 17.1$ Hz, 10.3, 2H), 4.32 (q, $J = 6.8$ Hz, 1H), 4.14 (q, $J = 4.6$ Hz, 2.4 Hz, 1H), 4.09 (dd, $J = 8.1$ Hz, 6.1 Hz, 1H), 3.85 (t, $J = 7.7$ Hz, 1H), 3.04 (d, $J = 4.6$ Hz, 1H), 2.61–2.56 (m, 1H), 1.47 (s, 9H), 1.43 (s, 3H), 1.37 (s, 3H). $^{13}\text{C NMR}$ (100 MHz, CDCl_3) δ 172.5, 132.4, 119.6, 109.1, 82.7, 76.0, 71.2, 67.3, 50.3, 27.9, 26.8, 25.4. LRMS-ESI (m/z) 295 (M+Na).

(2R,3S)-*t*-Butyl 2-(benzyloxy)-3-((S)-2,2-dimethyl-1,3-dioxolan-4-yl)pent-4-enoate (8)

To a cold (0 °C) solution of **7** (4.1 g, 14.9 mmol), benzyl bromide (2.30 mL, 19.37 mmol) and tetrabutyl ammonium iodide (0.50 g, 1.50 mmol) in THF (50.0 mL) was added sodium hydride (0.78 g, 19.37 mmol). The reaction was warmed to 23 °C and allowed to stir for 3 h. Upon completion the reaction was quenched with saturated ammonium chloride (10.0 mL). The reaction was extracted with ethyl acetate (3×10 mL). The organic layers were combined, washed with brine and dried over anhydrous sodium sulfate. The solvent was reduced under vacuum and the residue was purified on silica gel to obtain **8** (5.3 g, 99% yield) as a colorless oil. $R_f = 0.61$ (20% ethyl acetate/hexanes). $^1\text{H NMR}$ (400 MHz, CDCl_3)

δ 7.35–7.29 (m, 5H), 5.95–5.85 (m, 1H), 5.18 (dd, $J = 17.2, 10.3$ Hz, 2H) 4.75 (d, $J = 11.5$ Hz, 1H), 4.33 (d, $J = 11.5$ Hz, 1 H), 4.20 (q, $J = 7.3$, 1H), 3.85 (d, $J = 3.5$ Hz, 1H), 3.77 (dd, $J = 6.1, 2.0$ Hz, 1H), 3.66 (t, $J = 7.7$ Hz, 1H), 2.64–2.58 (m, 1H), 1.47 (s, 9H), 1.39 (s, 3H), 1.33 (s, 3H). ^{13}C NMR (100 MHz, CDCl_3) δ 169.9, 137.3, 133.5, 128.3, 128.2, 127.9, 119.1, 108.9, 81.7, 78.2, 75.6, 72.3, 67.2, 50.3, 28.1, 26.6, 25.4. LRMS-ESI (m/z) 385 (M+Na).

(3S,3aS,4R,6aR)-4-(Benzyloxy)hexahydrofuro[2,3-b]furan-3-ol (9)

To a cold (0 °C) solution of **8** (5.3 g, 14.8 mmol) in THF (50.0 mL) was added lithium aluminum hydride (1.3 g, 31.3 mmol). The reaction was allowed to stir for 1 h at 23 °C after which the reaction was cooled to 0 °C and quenched by adding excess ethyl acetate, 1 N NaOH (0.5 mL), H_2O (0.5 mL). After a white precipitate formed magnesium sulfate was added and stirred for 15 min. The reaction mixture was filtered and concentrated under vacuum.

The crude mixture was taken up in $\text{CH}_2\text{Cl}_2/\text{MeOH}$ (20.0 ml, 4:1), cooled to –78 °C and a stream of O_3 was bubbled through the solution until a blue color persisted. Upon consumption of the starting material, argon was bubbled through the blue solution until the solution became clear. Dimethyl sulfide (0.13 mL, 1.75 mmol) was added to the reaction and the mixture was warmed to room temperature and stirred an additional 3 h. The reaction mixture was carefully concentrated at (0 °C), then 5 mL of CH_2Cl_2 , p-TsOH (30.0 mg) and MeOH (0.5 μL) were added to the residue and the mixture was stirred for 6 h at room temperature. The reaction was again carefully concentrated and the residue was purified on silica gel (20% ether/hexanes to 50% ether/hexanes) to afford compound **9**, (1.5 g, 42 % yield 2 steps) as a colorless oil. $R_f = 0.52$ (60% ethyl acetate/hexanes). ^1H NMR (400 MHz, CDCl_3) δ 7.38–7.29 (m, 5H), 5.82 (d, $J = 5.3$ Hz, 1H), 4.56–4.46 (m, 4H), 4.12 (d, $J = 10.2$ Hz, 1H), 4.03 – 3.96 (m, 2H) 3.61 – 3.57 (dd, $J = 6.9, 6.8$ Hz, 1H), 2.91 (dd, $J = 5.3, 5.4$ Hz, 1H), 2.16 (bs, 1H). ^{13}C NMR (100 MHz, CDCl_3) δ 137.7, 128.4, 127.7, 127.7, 109.2, 78.6, 74.2, 73.2, 71.1, 68.9, 55.4. LRMS-ESI (m/z) 237 (M+H).

(3R,3aS,4R,6aR)-3-Azido-4-(benzyloxy)hexahydrofuro[2,3-b]furan (10)

To a cold (0 °C) solution of **9** (0.18 g, 0.76 mmol) and triphenylphosphine (0.40 g, 1.52 mmol) in THF (5.0 mL) was added diethyl azodicarboxylate (40 % in toluene) (0.66 mL, 1.52 mmol) followed by diphenylphosphoryl azide (0.33 mL, 1.52 mmol). The reaction was allowed to stir 18 h before diluting with ethyl acetate (10 mL) and quenched with a saturated solution of sodium bicarbonate (10 mL). The reaction was extracted with ethyl acetate (3 \times 15 ml). The organic layers were combined, washed with brine and dried over anhydrous sodium sulfate. The solvent was concentrated under vacuum and the crude mixture was purified on silica gel using 5% ethyl acetate/hexanes to obtain **10** (0.15 g, 73% yield) as colorless oil. ^1H NMR (400 MHz, CDCl_3) δ 7.45 – 7.23 (m, 5H), 5.79 (d, $J = 5.1$ Hz, 1H), 4.55 (d, $J = 5.1$ Hz, 2H), 4.41 – 4.35 (d, $J = 4.3$ Hz, 1H), 4.32 – 4.21 (m, 1H), 4.10 (dd, $J = 10.1$ Hz, 4.4 Hz, 1H), 4.04 – 3.94 (m, 2H), 3.65 (dd, $J = 9.2, 7.9$, 1H), 2.97 – 2.93 (m, 1H). ^{13}C NMR (100 MHz, CDCl_3) δ 137.0, 128.6, 128.1, 127.7, 108.6, 76.6, 73.9, 72.7, 70.8, 61.2, 51.8.

(3*R*,3*aS*,4*R*,6*aR*)-4-Azidohexahydrofuro[2,3-*b*]furan-3-ol (11)

Benzyl ether **10** (124 mg, 0.47 mmol) was dissolved in dry DCM under argon. K₂CO₃ (164 mg, 1.19 mmol, 2.5 eq) was added and stirred for 30 minutes at room temperature. The reaction was cooled to -78°C and BBr₃ (1 M in DCM, 0.52 mL, 0.52 mmol, 1.1 eq) was added dropwise. The reaction was allowed to warm slowly from -78°C to -20°C and then maintained at -20°C for a total of 2 hours. Upon consumption of starting material identified via TLC analysis, the crude reaction mixture was loaded onto a column and was purified via flash column chromatography on silica gel (30% ethyl acetate/hexanes to 50% ethyl acetate/hexanes) to afford compound **11** (51 mg, 64%) as a yellow residue. R_f = 0.13 (30% ethyl acetate/hexanes) ¹H NMR (400 MHz, CDCl₃) δ 5.78 (d, *J* = 5.2 Hz, 1H), 4.60–4.52 (m, 1H), 4.41 (dt *J* = 4.7, 6.1 Hz, 1H), 4.09 (dd, *J* = 10.1, 4.4 Hz, 1H), 4.03–3.96 (m, 2H), 3.63 (dd, *J* = 9.6, 6.6 Hz, 1H) 2.91–2.85 (m, 1H) ¹³C NMR (100 MHz, CDCl₃) δ 108.8, 74.0, 73.2, 69.9, 60.9, 53.2. LRMS-ESI (*m/z*) 237 (M+H).

***t*-Butyl (3*R*,3*aS*,4*R*,6*aR*)-4-(benzyloxy)hexahydrofuro[2,3-*b*]furan-3-ylcarbamate (12)**

To a round bottom flask charged with **10** (0.09 g, 0.36 mmol) and Boc₂O (0.09 g, 0.43 mmol) in ethyl acetate (5.0 mL) (under argon) was added 10% Pd/C (10% by wt.). The mixture was stirred under an atmosphere of hydrogen for 18 h at 1 atm. Upon completion the reaction mixture was filtered through a plug of silica. The solvent was concentrated under vacuum and purified on silica gel using 20% ethyl acetate/hexanes to obtain **12** (0.12 g, 98% yield) as white solid. R_f = 0.61 (40% ethyl acetate/hexanes). ¹H NMR (300 MHz, CDCl₃) δ 7.48 – 7.26 (m, 5H), 5.76 (d, *J* = 5.2 Hz, 1H), 4.90 – 4.67 (m, 2H), 4.55 (d, *J* = 11.6, 2H), 4.24 (dd, *J* = 15.8, 7.2, 1H), 4.06 (dd, *J* = 9.7, 4.4, 1H), 3.96 (dd, *J* = 9.4, 6.7, 1H), 3.84 (d, *J* = 9.7, 1H), 3.69 (dd, *J* = 9.3, 7.5, 1H), 2.85 – 2.81 (m, 1H), 1.45 (s, 9H). ¹³C NMR (75 MHz, CDCl₃) δ 155.0, 137.5, 128.5, 127.9, 108.7, 79.7, 76.8, 75.3, 72.5, 71.3, 52.8, 52.4, 28.4. LRMS-ESI (*m/z*) 358 (M+Na).

Methyl (3*R*,3*aS*,4*R*,6*aR*)-4-(benzyloxy)hexahydrofuro[2,3-*b*]furan-3-ylcarbamate (13)

(3*R*,3*aS*,4*R*,6*aR*)-3-azido-4-(benzyloxy)hexahydrofuro[2,3-*b*]furan (**10**) (0.05 g, 0.19 mmol) and triphenyl phosphine (0.06 g, 0.230 mmol) was dissolved in THF/H₂O (4.0 mL, 3:1) and stirred at 23 °C for 24 h. After the consumption of the starting material, saturated sodium bicarbonate (1.0 mL) was added followed by methyl chloroformate (0.05 mL, 0.65 mmol) and the reaction was stirred for 6 h. The reaction was diluted and extracted with ethyl acetate (3×5 mL). The organic layers were combined, washed with brine and concentrated under vacuum. The crude mixture was purified on silica gel using 20 % ethyl acetate/hexanes to obtain **13** (40.0 mg, 71% yield). R_f = 0.24 (20 % ethyl acetate/hexanes). ¹H NMR (300 MHz, CDCl₃) δ 7.46 – 7.23 (m, 5H), 5.77 (d, *J* = 5.2 Hz, 1H), 5.15 (d, *J* = 7.4 Hz, 1H), 4.79 (d, *J* = 11.5 Hz, 1H), 4.59–4.53 (m, 2H), 4.25 (dd, *J* = 15.8 Hz, 7.6 Hz, 1H), 4.06 (dd, *J* = 9.9 Hz, 4.4 Hz, 1H), 3.98 (dd, *J* = 9.3 Hz, 6.8 Hz, 1H), 3.86 (d, *J* = 9.9 Hz, 1H), 3.68 (s, 4H), 2.93 – 2.79 (m, 1H). ¹³C NMR (75 MHz, CDCl₃) δ 156.3, 137.4, 128.5, 127.9, 108.6, 76.8, 75.0, 72.5, 71.3, 52.8, 52.1

***t*-Butyl (3*R*,3*aS*,4*R*,6*aR*)-4-(benzyloxy)hexahydrofuro[2,3-*b*]furan-3-yl(methyl)carbamate (14)**

To a cold (0 °C) solution of **12** (0.03 g, 0.10 mmol) in THF (5.0 mL) was added NaH (0.01 g, 0.19 mmol) and methyl iodide (12.0 μ L, 0.19 mmol). The mixture was warmed to room temperature and stirred for 2 h. Upon completion, the solution was cooled to 0 °C and saturated ammonium chloride (1.0 mL) was added. The reaction was diluted and extracted with ethyl acetate (3 \times 15 ml). The organic layers were combined, washed with brine and dried over anhydrous sodium sulfate. The solvent was concentrated under vacuum and the crude mixture was purified on silica gel using 20% ethyl acetate/hexanes to obtain **14** (34.0 mg, 98% yield). R_f = 0.48 (40% ethyl acetate/hexanes). $^1\text{H NMR}$ (300 MHz, CDCl_3) δ 7.64 – 7.23 (m, 5H), 5.81 (d, J = 5.3 Hz, 1H), 5.44 – 5.01 (m, 1H), 4.70 (bs, 1H), 4.49 (d, J = 11.7 Hz, 1H), 4.23 (dd, J = 15.0 Hz, 8.3 Hz, 1H), 4.11 (dd, J = 10.1 Hz, 6.3 Hz, 1H), 4.01 – 3.89 (m, 2H), 3.63 (t, J = 8.6 Hz, 1H), 2.86 (bs, 1H), 2.81 (s, 3H), 1.45 (s, 9H). $^{13}\text{C NMR}$ (75 MHz, CDCl_3) δ 155.1, 137.5, 128.4, 127.8, 109.2, 80.0, 76.5, 74.0, 72.4, 70.43, 52.9, 52.4, 50.6, 30.0, 28.4.

***t*-Butyl (3*R*,3*aS*,4*R*,6*aR*)-4-(benzyloxy)hexahydrofuro[2,3-*b*]furan-3-yl(ethyl)carbamate (15)**

To a round bottom flask charged with activated molecular sieves (0.5g) was added DMF (2.0 mL), **12** (0.29g, 0.86 mmol), ethyl iodide (0.15 mL, 1.82 mmol) and $\text{CsOH}\cdot\text{H}_2\text{O}$ (0.31g, 1.82 mmol). The mixture was heated to 60 °C for 12 h. Upon completion, the reaction mixture was diluted with ethyl acetate and filtered through a plug of celite. The organic layer was washed with water and dried over anhydrous sodium sulfate. After purification by flash chromatography the product (**15**) was obtained as a white solid (284 mg, 91 % yield). R_f = 0.45 (20 % ethyl acetate/hexanes). $^1\text{H NMR}$ (400 MHz, CDCl_3) δ 7.42 – 7.28 (m, 5H), 5.81 (d, J = 5.2 Hz, 1H), 4.94 (bs, 1H), 4.69 (d, J = 11.0 Hz, 1H), 4.50 (d, J = 11.7 Hz, 1H), 4.24 – 4.18 (m, 1H), 4.13 (dd, J = 9.7, 6.9 Hz, 1H), 3.96 – 3.92 (m, 2H), 3.63 (t, J = 8.7 Hz, 1H), 3.33 – 3.15 (m, 2H), 3.00 – 2.98 (m, 1H) 1.46 (s, 9H), 1.14 (t, J = 7.0 Hz, 3H). $^{13}\text{C NMR}$ (100 MHz, CDCl_3) δ 154.8, 137.5, 128.4, 127.8, 127.6, 109.2, 79.7, 76.6, 74.0, 72.5, 70.1, 56.3, 51.1, 38.5, 28.4, 15.1

***t*-Butyl ((3*R*,3*aR*,4*R*,6*aR*)-4-(benzyloxy)hexahydrofuro[2,3-*b*]furan-3-yl) (isopropyl)carbamate (16)**

To a solution of azide (56.0 mg, 0.21 mmol) in ethyl acetate (2 mL) was added 10% Pd-C (5 mg) at 23 °C under argon. The argon balloon was replaced with a H_2 balloon, and the reaction mixture was stirred for 2 h under H_2 atmosphere. The reaction mixture was filtered through Celite, washed with ethyl acetate, and concentrated under reduced pressure, and the resulting residue was directly used for the next step.

To the crude amine, reagent grade acetone (0.25 mL, 3.0 mmol) was added and stirred for 24 h at room temperature. Acetone was removed by rotary evaporation and reconstituted with 100% ethanol (0.25 mL). To the resulting mixture was added NaBH_4 (16.0 mg, 0.42 mmol) and the reaction mixture stirred for an additional 2 h. The reaction was then quenched with sat. NaHCO_3 and then extracted with CH_2Cl_2 (3 \times 2 mL). The combined extracts were dried over anhydrous Na_2SO_4 , filtered, and concentrated under reduced pressure.

Above crude isopropyl derivative was dissolved in CH_2Cl_2 , Et_3N (73 μL , 0.44 mmol) and di-*tert*-butyl dicarbonate (57.0 mg, 0.26 mmol) were added and stirred at room temperature overnight. The mixture is concentrated *in vacuo* and the residue was purified by silica gel column chromatography (15% EtOAc/hexanes) to obtain the product **16** 47.0 mg (yield 59%, over three steps). ^1H NMR (400 MHz, CDCl_3) δ 7.38–7.32 (m, 5H), 5.83 (d, J = 4.8 Hz, 1H), 4.77–4.58 (m, 1H), 4.63 (d, J = 12.1 Hz, 1H), 4.52 (d, J = 12.1 Hz, 1H), 4.22–4.12 (m, 2H), 3.98–3.84 (m, 3H), 3.67–3.59 (m, 1H), 3.09–3.02 (m, 1H), 1.48 (s, 9H), 1.19 (d, J = 6.9 Hz, 3H), 1.16 (d, J = 6.9 Hz, 3H); ^{13}C NMR (125 MHz, CDCl_3) δ 154.9, 137.6, 128.5, 128.0, 127.9, 109.7, 82.2, 80.1, 74.7, 72.7, 69.9, 51.3, 47.7, 29.7, 28.6; LRMS (ESI), m/z 378 ($\text{M} + \text{H}$) $^+$.

General Procedure for O-benzyl deprotection

To a round bottom flask charged with the indicated starting material (**12** – **16**) in methanol (5.0 mL) (under argon) was added $\text{Pd}(\text{OH})_2$ (10 mol%). The mixture was stirred under a 1 atm (hydrogen balloon) for 18 h. Upon completion the reaction mixture was filtered through a plug of silica. The solvent was concentrated under vacuum and the crude mixture was purified on silica gel using 20% – 30% ethyl acetate/hexanes to obtain the desired alcohols (**17**–**21**).

t-Butyl (3*R*,3*aS*,4*R*,6*aR*)-4-hydroxyhexahydrofuro[2,3-*b*]furan-3-ylcarbamate (**17**)

Following the general procedure outlined above, alcohol **17** was prepared in 95% yield. R_f = 0.24 (60 % ethyl acetate/hexanes). ^1H NMR (300 MHz, CDCl_3) δ 5.74 (d, J = 5.2, 1H), 4.97 (d, J = 8.7 Hz, 1H), 4.60 – 4.41 (m, 2H), 4.15 (dd, J = 9.6 Hz, 5.8 Hz, 1H), 4.03 (dd, J = 9.0 Hz, 6.8 Hz, 1H), 3.73 (dd, J = 9.7 Hz, 2.9 Hz, 1H), 3.60 (t, J = 8.6 Hz, 1H), 2.74 (s, 1H), 2.1 (bs, 1H) 1.43 (s, 9H). ^{13}C NMR (75 MHz, CDCl_3) δ 155.9, 109.1, 80.5, 73.5, 72.7, 69.9, 55.3, 50.9, 28.3

Methyl (3*R*,3*aS*,4*R*,6*aR*)-4-hydroxyhexahydrofuro[2,3-*b*]furan-3-ylcarbamate (**18**)

Following the general procedure outlined above, alcohol **18** was prepared in 72% yield. R_f = 0.16 (60 % ethyl acetate/hexanes). ^1H NMR (300 MHz, CDCl_3) δ 5.76 (d, J = 5.2 Hz, 1H), 5.21 (bs, 1H), 4.66 – 4.44 (m, 2H), 4.16 (dd, J = 9.7 Hz, 5.6 Hz, 1H), 4.04 (dd, J = 9.0 Hz, 6.8 Hz, 1H), 3.89 (d, J = 3.2 Hz, 1H), 3.78 (dd, J = 9.8 Hz, 2.4 Hz, 1H), 3.72 – 3.53 (m, 4H), 2.87 – 2.65 (m, 1H). ^{13}C NMR (75 MHz, CDCl_3) δ 157.0, 109.04, 73.6, 72.9, 69.9, 55.1, 52.4, 51.5

t-Butyl (3*R*,3*aS*,4*R*,6*aR*)-4-hydroxyhexahydrofuro[2,3-*b*]furan-3-yl(methyl)carbamate (**19**)

Following the general procedure outlined above, alcohol **19** was prepared in 90% yield. R_f = 0.22 (60 % ethyl acetate/hexanes). ^1H NMR (300 MHz, CDCl_3) δ 5.77 (d, J = 5.1 Hz, 1H), 5.14 – 4.95 (m, 1H), 4.52 (d, J = 2.6 Hz, 1H), 4.29 – 3.84 (m, 4H), 3.57 (t, J = 8.7 Hz, 1H), 2.80 (s, 3H), 2.70 (bs, 1H), 1.46 (s, 9H). ^{13}C NMR (75 MHz, CDCl_3) δ 155.7, 109.0, 80.7, 72.6, 71.0, 70.2, 54.7, 53.9, 29.5, 28.4

***t*-Butyl ethyl((3*R*,3*aS*,4*R*,6*aR*)-4-hydroxyhexahydrofuro[2,3-*b*]furan-3-yl)carbamate (20)**

Following the general procedure outlined above, alcohol **20** was prepared in 81 % yield. $R_f = 0.25$ (40 % ethyl acetate/hexanes). $^1\text{H NMR}$ (400 MHz, CDCl_3) δ 5.75 (d, $J = 4.4$ Hz, 1H), 4.77 (bs, 1H), 4.43 – 4.37 (m, 1H), 4.02 (dd, $J = 10.2, 7.2$ Hz, 1H), 3.94 – 3.85 (m, 2H), 3.51 – 3.45 (m, 1H), 3.18 (dd, $J = 14.4, 7.1$ Hz, 1H), 3.30 (m, 1H), 3.03 (bs, 1H), 2.72 (bs, 1H) 1.37 (s, 9H), 1.14 (t, $J = 7.0$, 3H). $^{13}\text{C NMR}$ (100 MHz, CDCl_3) δ 154.0, 108.9, 80.5, 72.5, 71.1, 70.1, 55.1, 54.6, 38.8, 28.3, 15.5

***t*-Butyl ((3*R*,3*aS*,4*R*,6*aR*)-4-hydroxyhexahydrofuro[2,3-*b*]furan-3-yl)(isopropyl)carbamate (21)**

Following the general procedure outlined above, alcohol **21** was prepared in 95% yield. $^1\text{H NMR}$ (400 MHz, CDCl_3) δ 5.81 (d, $J = 5.1$ Hz, 1H), 4.88–4.64 (bs, 1H), 4.44 (quin, $J = 6.8, 13.8$ Hz, 1H), 4.17–4.09 (m, 1H), 4.01 (dd, $J = 6.4, 9.0$ Hz, 1H), 3.91 (dd, $J = 4.4, 9.7$ Hz, 1H), 3.65 (t, $J = 8.4$ Hz, 2H), 2.87–2.77 (bs, 1H), 1.49 (s, 9H), 1.26 (d, $J = 6.8$ Hz, 3H), 1.22 (d, $J = 6.8$ Hz, 3H); $^{13}\text{C NMR}$ (125 MHz, CDCl_3) δ 109.3, 80.7, 72.8, 71.3, 70.4, 53.7, 46.7, 28.5, 21.8, 21.4; LRMS (ESI), m/z 310 (M + Na) $^+$.

Preparation of activated carbonates **22a–f from polycyclic P_2 -ligands**

To a solution of the corresponding alcohol (**11**, **17** – **21**) in dry CH_2Cl_2 was added pyridine (2.3 eq). The resulting mixture was cooled to 0 °C under argon and 4-nitrophenylchloroformate (2.2 eq) was added in a single portion. The resulting mixture was warmed to 23 °C and stirred until the starting material was consumed. The reaction mixture was evaporated to dryness and the residue was purified by flash column chromatography on silica gel using a gradient of 20–40% ethyl acetate/hexanes to afford the desired ligand-activated carbonate **22a–f**.

(3*R*,3*aS*,4*R*,6*aR*)-4-Azidohexahydrofuro[2,3-*b*]furan-3-yl 4-nitrophenyl carbonate (22a)

Follow): Following the general procedure outlined above for the activation of the bis-THF alcohol, carbonate **22a** was obtained in 65% yield. $R_f = 0.53$, (40% ethyl acetate/hexanes). $^1\text{H NMR}$ (400 MHz, CDCl_3) δ 8.31 (d, $J = 8.0$ Hz, 2H), 7.40 (d, $J = 12.0$ Hz, 2H), 5.89 (d, $J = 5.2$ Hz, 1H), 5.39 – 5.34 (m, 1H), 4.32 (bs, 1H), 4.25 – 4.12 (m, 2H), 4.08 (d, $J = 10.3$ Hz, 1H), 3.96 (dd, $J = 10.3$ Hz, 5.6 Hz, 1H), 3.18 – 3.15 (m, 1H). $^{13}\text{C NMR}$ (100 MHz, CDCl_3) δ 154.9, 151.7, 145.6, 125.4, 121.6, 108.6, 76.1, 73.6, 70.6, 61.2, 51.7

***t*-Butyl(3*R*,3*aS*,4*R*,6*aR*)-4-((4-nitrophenoxy)carbonyloxy)hexahydrofuro[2,3-*b*]furan-3-ylcarbamate (22b)**

Following the general procedure outlined above for the activation of the bis-THF alcohol, carbonate **22b** was obtained in 86% yield. $R_f = 0.38$, (40% ethyl acetate/hexanes). $^1\text{H NMR}$ (300 MHz, CDCl_3) δ 8.20 (d, $J = 12.2$ Hz, 2H), 7.45 (d, $J = 12.0$ Hz, 2H), 5.83 (d, $J = 5.2$ Hz, 1H), 5.37 – 5.32 (m, 1H), 4.92 (d, $J = 8.2$ Hz, 1H), 4.54 (bs, 1H), 4.19 – 4.09 (m, 2H), 4.02 – 3.75 (m, 2H), 3.07 – 3.03 (m, 1H), 1.44 (s, 9H). $^{13}\text{C NMR}$ (75 MHz, CDCl_3) δ 155.2, 154.9, 151.8, 145.6, 125.3, 122.0, 108.5, 80.2, 76.3, 74.5, 70.7, 53.3, 51.9, 28.3. LRMS (ESI), m/z 433 (M + Na) $^+$.

Methyl(3*R*,3*aS*,4*R*,6*aR*)-4-((4-nitrophenoxy)carbonyloxy)hexahydrofuro[2,3-*b*]furan-3-yl)carbamate (22c)

Following the general procedure outlined above for the activation of the bis-THF alcohol, carbonate **22c** was obtained in 86% yield. $R_f = 0.52$, (40% ethyl acetate/hexanes). $^1\text{H NMR}$ (300 MHz, CDCl_3) δ 8.29 (d, $J = 12.0$ Hz, 2H), 7.45 (d, $J = 9.0$ Hz, 2H), 5.83 (d, $J = 5.2$ Hz, 1H), 5.33 (dt, $J = 8.5, 6.0$ Hz, 1H), 5.18 (d, $J = 8.2$ Hz, 1H), 4.56 (bs, 1H), 4.22 – 4.22 – 4.10 (m, 2H), 4.03 – 3.82 (m, 2H), 3.67 (s, 3H), 3.07 (t, $J = 8.6$, Hz, 1H). $^{13}\text{C NMR}$ (75 MHz, CDCl_3) δ 156.2, 155.2, 151.8, 145.6, 125.3, 121.9, 108.4, 77.2, 76.1, 74.28, 70.5, 53.1, 52.3. LRMS (ESI), m/z 391 ($\text{M} + \text{Na}$) $^+$.

***t*-Butylmethyl((3*R*,3*aS*,4*R*,6*aR*)-4-((4-nitrophenoxy)carbonyloxy)hexahydrofuro[2,3-*b*]furan-3-yl)carbamate (22d)**

Following the general procedure outlined above for the activation of the bis-THF alcohol, carbonate **22d** was obtained in 94% yield. $R_f = 0.49$, (40% ethyl acetate/hexanes). $^1\text{H NMR}$ (300 MHz, CDCl_3) δ 8.25 (d, $J = 12.1$ Hz, 2H), 7.52 (d, $J = 8.7$ Hz, 2H), 5.88 (d, $J = 5.3$ Hz, 1H), 5.28 (bs, 2H), 4.19 – 4.10 (m, 2H), 4.01 (d, $J = 10.4$ Hz, 1H), 3.88 (t, $J = 8.8$ Hz, 1H), 3.10 (t, $J = 8.0$ Hz, 1H), 2.79 (s, 3H), 1.42 (s, 9H). $^{13}\text{C NMR}$ (75 MHz, CDCl_3) δ 155.4, 155.2, 151.8, 145.5, 125.1, 122.3, 108.9, 80.2, 76.2, 72.8, 69.5, 54.8, 51.3, 29.4, 28.3

***t*-Butyl ethyl((3*R*,3*aS*,4*R*,6*aR*)-4-((4-nitrophenoxy)carbonyloxy)hexahydrofuro[2,3-*b*]furan-3-yl)carbamate (22e)**

Following the general procedure outlined above for the activation of the bis-THF alcohol, carbonate **22e** was obtained in 88% yield. $R_f = 0.56$, (30% ethyl acetate/hexanes). $^1\text{H NMR}$ (400 MHz, CDCl_3) δ 8.25 (d, $J = 8.8$ Hz, 2H), 7.47 (d, $J = 8.9$ Hz, 2H), 5.87 (d, $J = 5.2$ Hz, 1H), 5.30 (q, $J = 7.2$ Hz, 1H), 5.00 (bs, 1H), 4.18 – 4.12 (m, 2H), 4.00 (dd, $J = 10.2, 2.6$ Hz, 1H), 3.89 (dd, $J = 9.7, 7.4$ Hz, 1H), 3.26 – 3.16 (m, 3H), 1.44 (s, 9H), 1.16 (t, $J = 7.0$ Hz, 3H). $^{13}\text{C NMR}$ (100 MHz, CDCl_3) δ 155.3, 151.7, 145.5, 126.0, 125.1, 121.9, 115.5, 108.9, 80.2, 76.2, 72.8, 69.5, 55.7, 51.8, 28.3, 15.5. LRMS (ESI), m/z 461 ($\text{M} + \text{Na}$) $^+$.

***t*-Butyl isopropyl((3*R*,3*aS*,4*R*,6*aR*)-4-(((4-nitrophenoxy)carbonyl)oxy)hexahydrofuro[2,3-*b*]furan-3-yl)carbamate (22f)**

Following the general procedure outlined above for the activation of the bis-THF alcohol, carbonate **22f** was obtained in 64% yield. $^1\text{H NMR}$ (400 MHz, CDCl_3) δ 8.28 (d, $J = 9.2$ Hz, 2H), 7.46 (d, $J = 8.4$ Hz, 2H), 5.91 (d, $J = 6.0$ Hz, 1H), 5.28 (q, $J = 7.5, 15.0$ Hz, 1H), 4.27 – 4.15 (m, 2H), 3.98 – 3.92 (m, 1H), 3.91 – 3.85 (m, 1H), 3.31 – 3.21 (m, 1H), 1.45 (s, 9H), 1.26 (d, $J = 6.9$ Hz, 3H), 1.23 (d, $J = 6.9$ Hz, 3H).

General procedure for the synthesis of HIV-1-protease inhibitors

Hydroxyethylamine sulfonamide Isostere **23** or **24** was taken up in CH_3CN and cooled to 0 °C. *i*-Pr₂EtN (5eq, excess) was added, and the resulting solution was stirred for 5 min. The corresponding activated bis-THF ligand (from **22a–f**) was added and the resulting yellow solution was stirred at 23 °C until the reaction was complete (18–24 h). The reaction was concentrated under vacuum and the crude residue purified by flash column chromatography on silica gel to obtain the desired inhibitor.

(3R,3aR,4R,6aR)-4-Azidohexahydrofuro[2,3-b]furan-3-yl (2S,3R)-3-hydroxy-4-(N-isobutyl-4-methoxyphenylsulfonamido)-1-phenylbutan-2-ylcarbamate (25a)

The titled inhibitor was synthesized using the general procedure outlined above. The desired inhibitor was obtained as an amorphous white solid (94% yield). $R_f = 0.47$ (50% ethyl acetate/hexanes). $^1\text{H NMR}$ (300 MHz, Chloroform- d) δ 7.72 (d, $J = 8.9$ Hz, 2H), 7.39 – 7.10 (m, 5H), 6.99 (d, $J = 8.9$ Hz, 2H), 5.74 (d, $J = 5.1$ Hz, 1H), 5.16 – 4.91 (m, 2H), 4.02 – 3.89 (m, 2H), 3.88 (s, 3H), 3.79 (d, $J = 4.0$ Hz, 3H), 3.74 – 3.64 (m, 2H), 3.35 (s, 1H), 3.24 – 2.85 (m, 5H), 2.83 – 2.73 (m, 2H), 1.88 – 1.79 (m, 1H), 0.93 (d, $J = 6.6$ Hz, 3H), 0.89 (d, $J = 6.6$ Hz, 3H). $^{13}\text{C NMR}$ (75 MHz, CDCl_3) δ 163.1, 154.9, 137.6, 129.5, 129.3, 128.5, 126.8, 114.4, 108.6, 73.6, 72.8, 72.2, 71.0, 61.4, 58.9, 55.6, 55.2, 53.6, 52.0, 35.4, 27.3, 20.1, 19.9. Mass: HRMS (ESI), Calcd for $\text{C}_{28}\text{H}_{37}\text{N}_5\text{O}_8\text{S}$: m/z 626.2261 (M+Na), found m/z 626.2260 (M+Na).

(3R,3aS,4R,6aR)-4-Aminohexahydrofuro[2,3-b]furan-3-yl (2S,3R)-3-hydroxy-4-(N-isobutyl-4-methoxyphenylsulfonamido)-1-phenylbutan-2-ylcarbamate (25b)

Inhibitor **25a** was dissolved in ethyl acetate and treated with Pd/C and under a hydrogen balloon for 1 h. The reaction mixture was filtered through a plug of celite. The solution was concentrated under vacuum and the crude residue purified by flash column chromatography on silica gel to yield inhibitor **25b** as an amorphous white solid (71% yield). $R_f = 0.10$ (10% methanol/ CH_2Cl_2). $^1\text{H NMR}$ (300 MHz, Chloroform- d) δ 7.72 (d, $J = 8.8$ Hz, 2H), 7.38 – 7.11 (m, 5H), 6.99 (d, $J = 8.9$ Hz, 2H), 5.76 (d, $J = 5.1$ Hz, 1H), 5.06 (d, $J = 8.0$ Hz, 2H), 3.99 – 3.88 (m, 8H), 3.75 – 3.53 (m, 2H), 3.21 – 2.95 (m, 5H), 2.83 – 2.76 (m, 2H), 2.64 (d, $J = 8.7$ Hz, 1H), 2.23 (bs, 2H), 1.88 – 1.79 (m, 1H), 0.91 (dd, $J = 14.7, 6.6$ Hz, 6H). Mass: HRMS (ESI), Calcd for $\text{C}_{28}\text{H}_{39}\text{N}_3\text{O}_8\text{S}$: m/z 578.2535 (M+Na), found m/z 578.2527 (M+Na).

(3R,3aS,4R,6aR)-4-((2S,3R)-3-Hydroxy-4-(N-isobutyl-4-methoxyphenylsulfonamido)-1-phenylbutan-2-ylcarbamoyloxy)hexahydrofuro[2,3-b]furan-3-yl *t*-butyl carbamate (25c)

The titled inhibitor was synthesized using the general procedure outlined above. The desired inhibitor **25c** was obtained as an amorphous white solid (69% yield). $R_f = 0.3$ (50% ethyl acetate/hexanes). $^1\text{H NMR}$ (400 MHz, CDCl_3) δ 7.67 (d, $J = 8.7$ Hz, 2H), 7.31 – 7.19 (m, 5H), 6.97 (d, $J = 8.9$ Hz, 2H), 5.74 (d, $J = 5.0$ Hz, 1H), 5.24 – 5.02 (m, 2H), 4.86 (d, $J = 6.7$ Hz, 1H), 4.19 (bs, 1H), 3.98 – 3.91 (m, 2H), 3.86 (s, 3H), 3.80 – 3.69 (m, 3H), 3.20 – 2.61 (m, 7H), 1.99 – 1.70 (m, 1H), 1.42 (d, $J = 2.6$ Hz, 9H), 0.87 (dd, $J = 15.4, 6.5$ Hz, 6H). $^{13}\text{C NMR}$ (100 MHz, CDCl_3) δ 163.0, 155.2, 154.8, 137.5, 129.4, 128.5, 126.5, 114.3, 108.3, 79.8, 74.8, 72.2, 71.5, 65.8, 58.7, 55.6, 55.1, 53.6, 52.6, 52.0, 35.2, 30.2, 28.3, 27.2, 20.0, 19.8, 15.2. Mass: HRMS (ESI), Calcd for $\text{C}_{33}\text{H}_{47}\text{N}_3\text{O}_{10}\text{S}$: m/z 700.2880 (M+Na), found m/z 700.2865 (M+Na).

(3R,3aS,4R,6aR)-4-((2S,3R)-3-Hydroxy-4-(N-isobutyl-4-methoxyphenylsulfonamido)-1-phenylbutan-2-ylcarbamoyloxy)hexahydrofuro[2,3-b]furan-3-yl methyl carbamate (25d)

The titled inhibitor **25d** was synthesized using the general procedure outlined above. The desired inhibitor **25d** was obtained as an amorphous white solid (96% yield). $R_f = 0.11$ (50% ethyl acetate/hexanes). $^1\text{H NMR}$ (300 MHz, Chloroform- d) δ 7.69 (d, $J = 8.7$ Hz, 2H), 7.43

– 7.16 (m, 5H), 6.98 (d, $J = 8.9$ Hz, 2H), 5.75 (d, $J = 5.0$ Hz, 1H), 5.11 (bs, 2H), 4.95 (bs, 1H), 3.99 (d, $J = 6.1$ Hz, 2H), 3.87 (s, 5H), 3.83 – 3.52 (m, 6H), 3.23 – 2.64 (m, 8H), 1.97 – 1.66 (m, 1H), 0.88 (dd, $J = 12.0, 6.7$ Hz, 6H). ^{13}C NMR (100 MHz, Chloroform- d) δ 162.9, 156.1, 155.2, 137.6, 129.7, 129.4, 128.5, 126.5, 114.3, 108.3, 74.5, 72.3, 72.1, 71.2, 58.6, 55.5, 55.2, 53.5, 52.5, 52.2, 52.1, 35.2, 27.1, 20.0, 19.8. Mass: HRMS (ESI), Calcd for $\text{C}_{30}\text{H}_{41}\text{N}_3\text{O}_{10}\text{S}$: m/z 658.2410 (M+Na), found m/z 658.2429 (M+Na).

(3R,3aS,4R,6aR)-4-((2S,3R)-3-Hydroxy-4-(*N*-isobutyl-4-methoxyphenylsulfonamido)-1-phenylbutan-2-ylcarbamoyloxy)hexahydrofuro[2,3-*b*]furan-3-yl methyl *t*-butyl carbamate (25e)

The titled inhibitor was synthesized using the general procedure outlined above. The desired inhibitor **25e** was obtained as an amorphous white solid (78% yield). $R_f = 0.33$ (50% ethyl acetate/hexanes). ^1H NMR (300 MHz, Chloroform- d) δ 7.84 – 7.53 (m, 2H), 7.39 – 7.07 (m, 5H), 6.96 (d, $J = 8.8$ Hz, 2H), 5.78 (s, 1H), 5.14 (s, 2H), 4.96 – 4.34 (m, 1H), 4.13 – 4.01 (m, 3H), 3.87 (s, 6H), 3.69 – 3.37 (m, 1H), 3.16 – 2.59 (m, 9H), 1.64 – 1.52 (m, 1H), 1.45 (d, $J = 9.4$ Hz, 9H), 1.00 – 0.75 (m, 6H). Mass: HRMS (ESI), Calcd for $\text{C}_{34}\text{H}_{49}\text{N}_3\text{O}_{10}\text{S}$: m/z 692.3217 (M+H), found m/z 692.3205 (M+Na).

(3R,3aR,4R,6aR)-4-(Methylamino)hexahydrofuro[2,3-*b*]furan-3-yl(2S,3R)-3-hydroxy-4-(*N*-isobutyl-4-methoxyphenylsulfonamido)-1-phenylbutan-2-ylcarbamate (25f)

Inhibitor **25e** was dissolved in $\text{CH}_2\text{Cl}_2/\text{TFA}$ (4:1) at 0 °C and stirred for 2 h and then warmed to 23 °C. The reaction mixture was concentrated under vacuum and purified by flash column chromatography on silica gel. The desired inhibitor **25f** was obtained as an amorphous white solid (65% yield). $R_f = 0.20$ (10% methanol/ CH_2Cl_2). ^1H NMR (300 MHz, Chloroform- d) δ 7.71 (d, $J = 8.9$ Hz, 2H), 7.41 – 7.13 (m, 5H), 6.98 (d, $J = 8.9$ Hz, 2H), 5.72 (d, $J = 5.2$ Hz, 1H), 5.22 – 4.90 (m, 2H), 3.96 (dd, $J = 9.7, 6.2$ Hz, 1H), 3.87 (s, 5H), 3.84 – 3.62 (m, 3H), 3.22 – 2.89 (m, 5H), 2.79 (dt, $J = 21.8, 8.1$ Hz, 4H), 2.17 (s, 3H), 2.16 (s, 1H), 1.91 – 1.75 (m, 1H), 0.90 (dd, $J = 12.8, 6.6$ Hz, 6H). ^{13}C NMR (75 MHz, CDCl_3) δ 163.1, 155.3, 137.7, 129.6, 129.5, 129.3, 128.5, 126.6, 114.4, 108.8, 74.1, 72.7, 71.0, 60.4, 58.8, 55.6, 55.2, 53.6, 51.6, 35.4, 33.9, 27.3, 20.1, 19.9. Mass: HRMS (ESI), Calcd for $\text{C}_{29}\text{H}_{41}\text{N}_3\text{O}_8\text{S}$: m/z 592.2692 (M+Na), found m/z 592.2690 (M+Na).

(3R,3aS,4R,6aR)-4-(Methylamino)hexahydrofuro[2,3-*b*]furan-3-yl(2S,3R)-4-(4-amino-*N*-isobutylphenylsulfonamido)-3-hydroxy-1-phenylbutan-2-ylcarbamate (25g)

Inhibitor **25g** was obtained over two steps. Amine **24** was reacted with carbonate **22d** and the resulting Boc protected intermediate was dissolved in $\text{CH}_2\text{Cl}_2/\text{TFA}$ (4:1) at 0 °C and stirred for 2 h at 23 °C. The reaction mixture was concentrated under vacuum and purified by flash column chromatography on silica gel. The desired inhibitor **25g** was obtained as an amorphous white solid (65% yield). $R_f = 0.10$ (10% methanol/ CH_2Cl_2). ^1H NMR (300 MHz, Chloroform- d) δ 7.54 (d, $J = 8.6$ Hz, 2H), 7.36 – 7.16 (m, 5H), 6.69 (d, $J = 8.6$ Hz, 2H), 5.75 (d, $J = 5.1$ Hz, 1H), 5.30 – 5.05 (m, 2H), 4.19 (s, 2H), 3.97 (dd, $J = 9.7, 6.2$ Hz, 1H), 3.86 (d, $J = 3.6$ Hz, 4H), 3.71 (dq, $J = 11.1, 4.7$ Hz, 2H), 3.22 – 2.87 (m, 5H), 2.87 – 2.68 (m, 4H), 2.27 (s, 3H), 1.92 – 1.71 (m, 1H), 0.91 (dd, $J = 12.1, 6.6$ Hz, 6H). ^{13}C NMR

(75 MHz, CDCl₃) δ 155.2, 150.7, 137.8, 129.5, 129.3, 128.5, 126.6, 125.9, 114.0, 108.8, 73.5, 72.7, 72.6, 71.0, 67.9, 60.3, 58.8, 55.3, 53.7, 51.1, 35.5, found m/z 577.2679 (M+H).

***t*-Butylethyl((3*R*,3*aS*,4*R*,6*aR*)-4-(((2*S*,3*R*)-3-hydroxy-4-((*N*-isobutyl-4-methoxyphenyl)sulfonamido)-1-phenylbutan-2-yl)carbamoyl)oxy)hexahydrofuro[2,3-*b*]furan-3-yl)carbamate (25h)**

The titled inhibitor was synthesized using the general procedure outlined above. The desired inhibitor **25h** was obtained as an oil (56% yield). R_f = 0.38 (50% ethyl acetate/hexanes). ¹H NMR (500 MHz, CDCl₃) δ 7.72 (m, 2H), 7.29 (m, 3H), 7.22 (m, 2H), 6.97 (d, J = 8.8 Hz, 2H), 5.80 (m, 1H), 5.13 (m, 1H), 4.04 (m, 1H), 3.91 (d, J = 9.7 Hz, 2H), 3.87 (s, 3H), 3.84 (bs, 2H), 3.69 (m, 1H), 3.19–2.87 (m, 8H), 2.76 (dd, J = 13.3 Hz, J = 6.6 Hz, 2H), 1.80 (m, 1H), 1.45 (s, 9H), 0.90 (d, J = 6.6 Hz, 3H), 0.86 (d, J = 6.4 Hz, 3H); ¹³C NMR (125 MHz, CDCl₃) δ 163.2, 155.5, 155.0, 137.7, 129.9, 129.7, 129.6, 128.7, 126.8, 114.5, 109.1, 80.3, 73.6, 72.6, 72.4, 70.8, 58.9, 55.8, 55.2, 53.8, 35.4, 28.6, 27.4, 20.3, 20.0, 15.8; LRMS-ESI (m/z) 728.6 [M + Na]⁺; HRMS-ESI (m/z) [M + Na]⁺ calcd for (C₃₅H₅₁N₃O₁₀S), 728.3193; found, 728.3186.

((3*R*,3*aS*,4*R*,6*aR*)-4-(Ethylamino)hexahydrofuro[2,3-*b*]furan-3-yl (2*S*,3*R*)-3-hydroxy-4-((*N*-isobutyl-4-methoxyphenyl)sulfonamido)-1-phenylbutan-2-yl)carbamate (25i)

The titled inhibitor was obtained over two steps. First the *N*-Boc protected intermediate was obtained following the general procedure outlined above. The *N*-Boc protected intermediate to inhibitor **25i** was dissolved in a solution of CH₂Cl₂/TFA (4:1) and stirred at 23 °C for 2 h. The reaction mixture was concentrated and the residue was purified by flash chromatography. Inhibitor **25i** was obtained as an amorphous white solid (62% yield, 2 steps). ¹H NMR (400 MHz, CD₄OD) δ 7.77 (d, J = 8.9 Hz, 2H), 7.28 (bs, 4H), 7.23 – 7.20 (m, 1H), 7.08 (d, J = 8.9 Hz, 2H), 5.73 (d, J = 5.2 Hz, 1H), 5.09 – 5.04 (m, 1H), 4.08 (d, J = 11.5 Hz, 1H), 4.00 – 3.93 (m, 3H), 3.87 (s, 3H), 3.85 – 3.82 (m, 1H), 3.81 – 3.71 (m, 2H), 3.50 (dd, J = 15.0, 3.8 Hz, 1H), 3.20 – 3.18 (m, 1H), 3.16 – 3.06 (m, 4H), 2.91 – 2.78 (m, 3H), 2.60 – 2.52 (m, 2H), 2.03 – 1.99 (m, 1H), 1.19 (t, J = 7.2 Hz, 3H), 0.90 (d, J = 5.5 Hz, 4H), 0.85 (d, J = 6.6 Hz, 3H). ¹³C NMR (75 MHz, CDCl₃) δ 163.1, 155.3, 137.9, 129.4, 128.5, 126.7, 114.3, 108.5, 72.1, 71.1, 60.3, 58.7, 58.4, 55.6, 53.2, 48.7, 41.4, 35.1, 29.6, 27.1, 21.0, 20.0, 19.8, 14.1. Mass: HRMS (ESI), Calcd for: C₃₀H₄₃N₃O₈S m/z 606.2849 (M + H), found m/z 606.2849 (M+H).

(3*R*,3*aS*,4*R*,6*aR*)-4-(Isopropylamino)hexahydrofuro[2,3-*b*]furan-3-yl ((2*S*,3*R*)-3-hydroxy-4-((*N*-isobutyl-4-methoxyphenyl)sulfonamido)-1-phenylbutan-2-yl)carbamate (25j)

The titled inhibitor was synthesized using the general procedure outlined above. The desired inhibitor **25j** was obtained as an amorphous white solid (73% yield). R_f = 0.4 (4% MeOH/CH₂Cl₂). ¹H NMR (400 MHz, CDCl₃) δ 7.69 (d, J = 9.0 Hz, 2H), 7.32–7.26 (m, 2H), 7.25–7.19 (m, 3H), 6.98 (d, J = 9.0 Hz, 2H), 5.73 (d, J = 5.6, 1H), 5.11 (q, J = 14.0, 7.1 Hz, 1H), 5.0 (d, J = 8.1 Hz, 1H), 4.0–3.93 (m, 1H), 3.92–3.82 (m, 3H), 3.87 (s, 3H), 3.79–3.68 (m, 3H), 3.27–3.23 (m, 1H), 3.17–3.08 (m, 1H), 3.05–2.87 (m, 5H), 2.82–2.69 (m, 3H), 1.87–1.76 (m, 1H), 0.99 (d, J = 6.2 Hz, 3H), 0.96 (d, J = 6.2 Hz, 3H), 0.91 (d, J = 6.6 Hz, 3H), 0.87 (d, J = 6.6 Hz, 3H); ¹³C NMR (125 MHz, CDCl₃) δ 163.3, 155.7, 137.6, 129.9,

129.7, 129.6, 128.8, 126.9, 114.6, 108.9, 75.1, 73.1, 72.8, 71.3, 59.0, 56.1, 55.8, 55.4, 53.8, 52.3, 46.3, 35.5, 27.5, 23.3, 23.1, 20.3, 20.1; HRMS-ESI (m/z) [$M + H$]⁺ calcd for ($C_{31}H_{45}N_3O_8S$), 620.3006; found, 620.2996.

(3R,3aS,4R,6aR)-4-(Dimethylamino)hexahydrofuro[2,3-b]furan-3-yl (2S,3R)-3-hydroxy-4-(N-isobutyl-4-methoxyphenylsulfonamido)-1-phenylbutan-2-ylcarbamate (25k)

Inhibitor **25k** (27 mg, 0.05 mmol) was dissolved in dichloroethane (2 mL) and paraformaldehyde (powder, 60 mg, excess), $NaBH_3CN$ (50 mg, 0.23 mmol) and AcOH (20 μ L) were added sequentially. The reaction mixture was stirred at 23 °C for 24 h. The reaction was diluted with CH_2Cl_2 and washed with sat. $NaHCO_3$. The organic layer was combined dried over magnesium sulfate and concentrated under vacuum and purified over silica gel. The desired inhibitor **25k** was obtained as an amorphous white solid (50% yield). $R_f = 0.33$ (10% methanol/ CH_2Cl_2). 1H NMR (300 MHz, Chloroform- d) δ 7.71 (d, $J = 8.8$ Hz, 2H), 7.38 – 7.12 (m, 5H), 6.99 (d, $J = 8.8$ Hz, 2H), 5.68 (d, $J = 5.3$ Hz, 1H), 5.18 – 5.13 (m, 1H), 5.04 (d, $J = 8.4$ Hz, 1H), 4.06 – 3.78 (m, 8H), 3.78 – 3.57 (m, 1H), 3.18 – 2.76 (m, 8H), 2.07 (s, 6H), 1.93 – 1.69 (m, 1H), 0.89 (dd, $J = 12.8, 6.6$ Hz, 6H). ^{13}C NMR (75 MHz, $CDCl_3$) δ 163.1, 155.2, 137.5, 129.6, 129.4, 129.3, 128.6, 126.7, 114.4, 109.2, 77.2, 72.8, 72.7, 72.6, 70.5, 64.7, 58.8, 55.6, 55.2, 53.7, 45.4, 41.4, 35.3, 27.3, 20.1, 19.8. Mass: HRMS (ESI), Calcd for $C_{30}H_{43}N_3O_8S$: m/z 606.2849 (M+Na), found m/z 606.2849 (M+Na).

(3R,3aS,4R,6aR)-4-(Diethylamino)hexahydrofuro[2,3-b]furan-3-yl (2S,3R)-3-hydroxy-4-(N-isobutyl-4-methoxyphenylsulfonamido)-1-phenylbutan-2-ylcarbamate (25l)

Inhibitor **25l** (27 mg, 0.05 mmol) was dissolved in dichloroethane (2 mL) and acetaldehyde (10 μ L, excess), $NaBH_3CN$ (50 mg, 0.23 mmol) and AcOH (20 μ L) were added sequentially. The reaction mixture was stirred at 23 °C for 24 h. The reaction was diluted with CH_2Cl_2 and washed with sat. $NaHCO_3$. The organic layer was combined dried over magnesium sulfate and concentrated under vacuum and purified over silica gel. The desired inhibitor **25l** was obtained as an amorphous white solid (53% yield). $R_f = 0.38$ (10% methanol/ CH_2Cl_2). 1H NMR (300 MHz, Chloroform- d) δ 7.69 (d, $J = 8.8$ Hz, 2H), 7.39 – 7.13 (m, 5H), 6.98 (d, $J = 8.9$ Hz, 2H), 5.69 (d, $J = 5.3$ Hz, 1H), 5.17 (d, $J = 8.3$ Hz, 1H), 5.02 (d, $J = 8.2$ Hz, 1H), 4.01 – 3.91 (m, 3H), 3.87 (s, 5H), 3.65 (dd, $J = 9.5, 6.4$ Hz, 1H), 3.56 (d, $J = 6.0$ Hz, 1H), 3.23 – 3.04 (m, 1H), 3.04 – 2.71 (m, 7H), 2.54 – 2.45 (m, 2H), 2.28 (m, 2H), 1.94 – 1.72 (m, 1H), 0.99 (t, $J = 7.1$ Hz, 6H), 0.88 (dd, $J = 11.3, 6.6$ Hz, 6H). ^{13}C NMR (75 MHz, $CDCl_3$) δ 163.0, 155.3, 137.3, 129.6, 129.4, 129.3, 128.6, 126.7, 114.3, 109.3, 73.4, 73.0, 72.4, 70.7, 60.7, 58.7, 55.6, 55.0, 53.6, 46.7, 43.9, 35.1, 27.2, 20.1, 19.9, 13.5. Mass: HRMS (ESI), Calcd for $C_{32}H_{47}N_3O_8S$: m/z 634.3162 (M+Na), found m/z 634.3152 (M+Na).

Methods: Determination of X-ray structures of HIV-1 protease-inhibitor complexes

The optimized HIV-1 protease was expressed and purified as described.³⁹ The protease-inhibitor complex was crystallized by the hanging drop vapor diffusion method with well solutions containing sodium chloride and sodium acetate buffer at pH 5. Diffraction data were collected on a single crystal cooled to 90 K at SER-CAT (using the 22-ID beamline for

inhibitor **25f** and the 22-BM beamline for inhibitor **25g**, Advanced Photon Source, Argonne National Lab (Chicago, USA) with X-ray wavelengths of 0.8 and 1.0 Å, respectively. X-ray data were processed by HKL-2000 with Rmerge values of 5.7% and 7.7%, respectively.⁴⁰ Using the isomorphous structure⁴¹ as an initial model, the crystal structures were solved with PHASER⁴² in CCP4i Suite,^{43,44} and refined with SHELX-97,⁴⁵ to 1.34 Å and 1.29 Å resolution, respectively, for the complexes with inhibitor **25f** and inhibitor **25g**. COOT,⁴⁶ was used for manual modification of the structures. PRODRG-2,⁴⁷ was used to construct the inhibitor and the restraints for refinement. Alternative conformations were modeled when visible in the electron density maps, and isotropic atomic displacement parameters (B factors) were applied for all atoms including solvent molecules. The final refined solvent structure comprised two sodium ions, three chloride ions and 147 water molecules for the protease complex with inhibitor **25f**, and one sodium ion, two chloride ions, three acetate ions and 137 water molecules for the complex with inhibitor **25g**. The crystallographic statistics are listed in the supplementary material section. The coordinates and structure factors of HIV-1 protease with inhibitor **25f** and inhibitor **25g** structures have been deposited in Protein Data Bank with code 5BR Y and 5BS4, respectively.

Acknowledgments

This research was supported by the National Institutes of Health (Grant GM53386, AKG and Grant GM62920, ITW). X-ray data were collected at the Southeast Regional Collaborative Access Team (SER-CAT) beamline 22BM at the Advanced Photon Source, Argonne National Laboratory. Use of the Advanced Photon Source was supported by the US Department of Energy, Basic Energy Sciences, Office of Science, under Contract No. W-31-109-Eng-38. This work was also supported by the Intramural Research Program of the Center for Cancer Research, National Cancer Institute, National Institutes of Health, and in part by a Grant-in-Aid for Scientific Research (Priority Areas) from the Ministry of Education, Culture, Sports, Science, and Technology of Japan (Monbu Kagakusho), a Grant for Promotion of AIDS Research from the Ministry of Health, Welfare, and Labor of Japan, and the Grant to the Cooperative Research Project on Clinical and Epidemiological Studies of Emerging and Reemerging Infectious Diseases (Renkei Jigyō) of Monbu-Kagakusho. The authors would like to thank the Purdue University Center for Cancer Research, which supports the shared NMR and mass spectrometry facilities.

Abbreviations

THF	tetrahydrofuran
bis-THF	bis-tetrahydrofuran
tris-THF	tris-tetrahydrofuran
PI	protease inhibitor
CNS	central nervous system
TFA	trifluoroacetic acid
DRV	darunavir
APV	amprenavir

References

1. Mitsuya H, Broder S. Strategies for antiviral therapy in AIDS. *Nature*. 1987; 325:773–778. [PubMed: 2434858]

2. Kohl NE, Emini EA, Schleif WA, Davis LJ, Heimbach JC, Dixon RAF, Scolnick EM, Sigal IS. Active human immunodeficiency virus protease is required for viral infectivity. *Proc Natl Acad Sci USA*. 1988; 85:4686–4690. [PubMed: 3290901]
3. Montaner JSG, Lima VD, Barrios R, Yip B, Wood E, Kerr T, Shannon K, Harrigan PR, Hogg RS, Daly P, Kendall P. Association of highly active antiretroviral therapy coverage, population viral load, yearly new HIV diagnoses in British Columbia, Canada: a population-based study. *Lancet*. 2010; 376:532–539. [PubMed: 20638713]
4. Braitstein P, Brinkhof MWG, Dabis F, Schechter M, Boulle A, Miotti P, Wood R, Laurent C, Sprinz E, Seyler C, Bangsberg DR, Balestre E, Sterne JAC, May M, Egger M, Grp A-L, Grp A-C. Mortality of HIV-1-infected patients in the first year of antiretroviral therapy: comparison between low-income and high-income countries. *Lancet*. 2006; 367:817–824. [PubMed: 16530575]
5. Este JA, Cihlar T. Current status challenges of antiretroviral research therapy. *Antiviral Res*. 2010; 85:25–33. [PubMed: 20018390]
6. Waters L, Nelson M. Why do patients fail HIV therapy? *Int J Clin Prac*. 2007; 61:983–990.
7. Moyle G, Back D. Principles practice of HIV-protease inhibitor pharmacoenhancement. *HIV Med*. 2001; 2:105–113. [PubMed: 11737387]
8. Kumar GN, Dykstra J, Roberts EM, Jayanti VK, Hickman D, Uchic J, Yao Y, Surber B, Thomas S, Granneman GR. Potent inhibition of the cytochrome P-450 3A-mediated human liver microsomal metabolism of a novel HIV protease inhibitor by ritonavir: A positive drug-drug interaction. *Drug Metab Dispos*. 1999; 27:902–908. [PubMed: 10421617]
9. van Sighem, AlvdW; Mark, A.; Ghani, Azra C.; Jambroes, Mariëlle; Reiss, Peter; Gyssens, Inge C.; Brinkman, Kees; Lange, Joep MA.; de Wolf, Frank. Mortality progression to AIDS after starting highly active antiretroviral therapy. *AIDS*. 2003; 17:2227–2326. [PubMed: 14523280]
10. Staszewski S, Morales-Ramirez J, Tashima KT, Rachlis A, Skiest D, Stanford J, Stryker R, Johnson P, Labriola DF, Farina D, Manion DJ, Ruiz NM. Efavirenz plus zidovudine lamivudine, efavirenz plus indinavir, and indinavir plus zidovudine lamivudine in the treatment of HIV-1 infection in adults. Study 006 Team. *N Eng J Med*. 1999; 341:1865–1873.
11. Wensing AM, van Maarseveen NM, Nijhuis M. Fifteen years of HIV Protease Inhibitors: raising the barrier to resistance. *Antiviral Res*. 2010; 85:59–74. [PubMed: 19853627]
12. Ghosh AK, Ramu Sridhar P, Kumaragurubaran N, Koh Y, Weber IT, Mitsuya H. Bis-tetrahydrofuran: a privileged ligand for darunavir a new generation of hiv protease inhibitors that combat drug resistance. *ChemMedChem*. 2006; 1:939–950. [PubMed: 16927344]
13. Ghosh AK, Sridhar PR, Leshchenko S, Hussain AK, Li J, Kovalevsky AY, Walters DE, Wedekind JE, Grum-Tokars V, Das D, Koh Y, Maeda K, Gatanaga H, Weber IT, Mitsuya H. Structure-based design of novel HIV-1 protease inhibitors to combat drug resistance. *J Med Chem*. 2006; 49:5252–5261. [PubMed: 16913714]
14. Ghosh, AK.; Chapsal, BD. Anti-HIV protease inhibitor Darunavir. In: Ganellin, CR.; Jefferis, R.; Roberts, S., editors. *Introduction to Biopharmaceuticals and Small Molecule Drug Research and Development: theory and case studies*. Elsevier; Waltham, MA: 2013. p. 355-384.
15. Ghosh AK, Dawson ZL, Mitsuya H. Darunavir a conceptually new HIV-1 protease inhibitor for the treatment of drug-resistant HIV. *Bioorg Med Chem*. 2007; 15:7576–7580. [PubMed: 17900913]
16. Ghosh, AK.; Chapsal, BD.; Mitsuya, H. Aspartic Acid Proteases as Therapeutic Targets. Ghosh, AK., editor. Vol. 45. Wiley-VCH; Weinheim: 2010. p. 205
17. Koh Y, Nakata H, Maeda K, Ogata H, Bilcer G, Devasamudram T, Kincaid JF, Boross P, Wang YF, Tie Y, Volarath P, Gaddis L, Harrison RW, Weber IT, Ghosh AK, Mitsuya H. Novel bis-tetrahydrofuranylurethane-containing nonpeptidic protease inhibitor (PI) UIC-94017 (TMC114) with potent activity against multi-PI-resistant human immunodeficiency virus in vitro. *Antimicrob Agents Chemother*. 2003; 47:3123–3129. [PubMed: 14506019]
18. De Meyer SAH, Surleraux D, Jochmans D, Tahri A, Pauwels R, Wigerinck P, de Bethune M. TMC 114, a novel human immunodeficiency virus type 1 protease inhibitor active against protease inhibitor-resistant viruses, including a broad range of clinical isolates. *Antimicrob Agents Chemother*. 2005; 49:2314–2321. [PubMed: 15917527]

19. Tie Y, Boross PI, Wang YF, Gaddis L, Hussain AK, Leshchenko S, Ghosh AK, Louis JM, Harrison RW, Weber IT. High resolution crystal structures of HIV-1 protease with a potent non-peptide inhibitor (UIC-94017) active against multi-drug-resistant clinical strains. *J Mol Biol.* 2004; 338:341–352. [PubMed: 15066436]
20. Ghosh AK, Anderson DD, Weber IT, Mitsuya H. Enhancing protein backbone binding—a fruitful concept for combating drug-resistant HIV. *Angew Chem Int Ed.* 2012; 51:1778–1802.
21. Ghosh AK, Chapsal BD, Weber IT, Mitsuya H. Design of HIV protease inhibitors targeting protein backbone: an effective strategy for combating drug resistance. *Acc Chem Res.* 2008; 41:78–86. [PubMed: 17722874]
22. Ghosh AK, Martyr CD, Steffey M, Wang YF, Agniswamy J, Amano M, Weber IT, Mitsuya H. Design of substituted bis-tetrahydrofuran (bis-THF)-derived potent HIV-1 protease inhibitors, protein-ligand X-ray structure, and convenient syntheses of bis-THF substituted bis-THF ligands. *ACS Med Chem Lett.* 2011; 2:298–302. [PubMed: 22509432]
23. Ghosh AK, Yashchuk S, Mizuno A, Chakraborty N, Agniswamy J, Wang YF, Aoki M, Gomez PM, Amano M, Weber IT, Mitsuya H. Design of gem-difluoro-bis-tetrahydrofuran as P2 ligand for HIV-1 protease inhibitors to improve brain penetration: synthesis, X-ray studies, and biological evaluation. *ChemMedChem.* 2015; 10:107–115. [PubMed: 25336073]
24. Salcedo Gomez PM, Amano M, Yashchuk S, Mizuno A, Das D, Ghosh AK, Mitsuya H. GRL-04810 and GRL-05010, difluoride-containing nonpeptidic HIV-1 protease inhibitors (PIs) that inhibit the replication of multi-PI-resistant HIV-1 in vitro and possess favorable lipophilicity that may allow blood-brain barrier penetration. *Antimicrob Agents Chemother.* 2013; 57:6110–6121. [PubMed: 24080647]
25. Al-Hakim AH, Haines AH, Morley C. Synthesis of 1,2-*O*-isopropylidene-L-threitol and its conversion to (*R*)-1,2-*O*-isopropylidene-glycerol. *Synthesis.* 1985; 1985:207–208.
26. Dueno EE, Chu F, Kim S-I, Jung KW. Cesium promoted *O*-alkylation of alcohols for the efficient ether synthesis. *Tetrahedron Lett.* 1999; 40:1843–1846.
27. Brückner R, Priepke H. Asymmetric induction in the [2,3]-Wittig rearrangement by chiral substituents in the allyl moiety. *Angew Chem Int Ed.* 1988; 27:278–280.
28. Brückner R. Asymmetric induction and simple diastereoselectivity in the [2,3]-Wittig rearrangement of ester enolates. *Chem Ber.* 1989; 122:703–710.
29. Swamy KCK, Kumar NNB, Balaraman E, Kumar KVP. Mitsunobu and related reactions: advances and applications. *Chem Rev.* 2009; 109:2551–2651. [PubMed: 19382806]
30. Ghosh AK, Bischoff A. A convergent synthesis of (+)-cryptophycin B, a potent antitumor macrolide from *Nostoc* sp. cyanobacteria. *Organic Lett.* 2000; 2:1573–1575.
31. Toth MV, Marshall GR. A simple, continuous fluorometric assay for HIV protease. *Int J Pept Protein Res.* 1990; 36:554–550.
32. Tie Y, Boross PI, Wang YF, Gaddis L, Hussain AK, Leshchenko S, Ghosh AK, Louis JM, Harrison RW, Weber IT. High resolution crystal structures of HIV-1 protease with a potent non-peptide inhibitor (UIC-94017) active against multi-drug-resistant clinical strains. *J Mol Biol.* 2004; 338:341–352. [PubMed: 15066436]
33. Miller MM, Liedtke MD, Lockhart SM, Rathbun RC. The role of dolutegravir in the management of HIV infections. *Infect Drug Resist.* 2015; 8:19–29. [PubMed: 25733917]
34. Mitsuya Y, Lie TF, Rhee SY, Fessel WJ, Shafter RW. Prevalence of darunavir resistance-associated mutations: patterns of occurrence and association with past treatment. *J Infect Dis.* 2007; 196:1177–1179. [PubMed: 17955436]
35. Koh Y, Amano M, Towata T, Danish M, Leshchenko-Yashchuk S, Das D, Nakayama M, Tojo Y, Ghosh AK, Mitsuya H. *In vitro* selection of highly darunavir-resistant-competent HIV-1 variants by using a mixture of clinical HIV-1 isolates resistant to multiple conventional protease inhibitors. *J Virol.* 2010; 84:11961–11969. [PubMed: 20810732]
36. Gatanaga H, Suzuki Y, Tsang H, Yoshimura K, Kavlick MF, Mardy S, Gorelick RJ, Tang C, Summers MF, Mitsuya H. Amino acid substitutions in non cleavage sites of the gag region are indispensable for high level HIV-1 resistance to protease inhibitors. *J Biol Chem.* 2002; 277:5952–5961. [PubMed: 11741936]

37. Koh Y, Aoki M, Danish ML, Aoki-Ogata H, Amano M, Das D, Shafer RW, Mitsuya H. Loss of protease dimerization inhibition activity of darunavir is associated with the acquisition of resistance to darunavir by HIV-1. *J Virol.* 2011; 85:10079–10089. [PubMed: 21813613]
38. Hayashi H, Takamune N, Nirasawa T, Aoki M, Morishita Y, Das D, Koh Y, Ghosh AK, Misumi S, Mitsuya H. Dimerization of HIV-1 protease occurs through two steps relating to the mechanism of protease dimerization inhibition by darunavir. *Proc Natl Acad Sci.* 2014; 79:5697–5709.
39. Mahalingam B, Louis JM, Hung J, Harrison RW, Weber IT. Structural implications of drug resistant mutants of HIV-1 protease: high resolution crystal structures of the mutant protease/substrate analog complexes. *Proteins.* 2001; 43:455–464. [PubMed: 11340661]
40. Otwinowski, Z.; Minor, W. Processing of X-ray diffraction data collected in oscillation mode. In: Carter, CW., Jr; Sweet, RM., editors. *Methods in Enzymology.* Vol. 276. Academic Press; New York: 1997. p. 307-326. *Macromolecular Crystallography, Part A*
41. Shen C-H, Wang Y-F, Kovalevsky AY, Harrison RW, Weber IT. Amprenavir complexes with HIV-1 protease and its drug-resistant mutants altering hydrophobic clusters. *FEBS J.* 2010; 277:3699–3714. [PubMed: 20695887]
42. McCoy AJ, Grosse-Kunstleve RW, Adams PD, Winn MD, Storoni LC, Read RJ. Phaser crystallographic software. *J Appl Crystallogr.* 2007; 40:658–674. [PubMed: 19461840]
43. Winn MD, et al. Overview of the CCP4 suite and current developments. *Acta Crystallogr Sect D: Biol Crystallogr.* 2011; 67:235–242. [PubMed: 21460441]
44. Potterton E, Briggs P, Turkenburg M, Dodson E. A graphical user interface to the CCP4 program suite. *Acta Crystallogr Sect D: Biol Crystallogr.* 2003; 59:1131–1137. [PubMed: 12832755]
45. Sheldrick GM. A short history of SHELX. *Acta Crystallogr Sect A: Found Crystallogr.* 2008; 64:112–122.
46. Emsley P, Lohkamp B, Scott WG, Cowtan K. Features and development of Coot. *Acta Crystallogr Sect D: Biol Crystallogr.* 2010; 66:486–501. [PubMed: 20383002]
47. Schuettelkopf AW, van Aalten DMF. PRODRG; a tool for high-throughput crystallography of protein-ligand complexes. *Acta Crystallogr Sect D: Biol Crystallogr.* 2004; 60:1355–1363. [PubMed: 15272157]

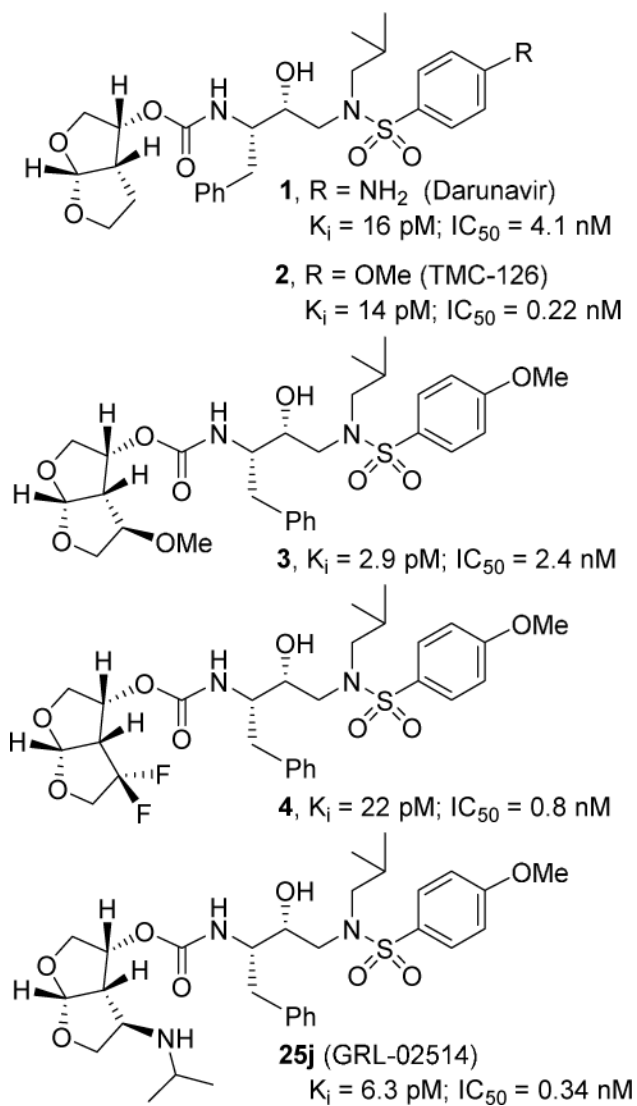


Figure 1.
Structure of HIV-1 protease inhibitors 1–4 and 25j.

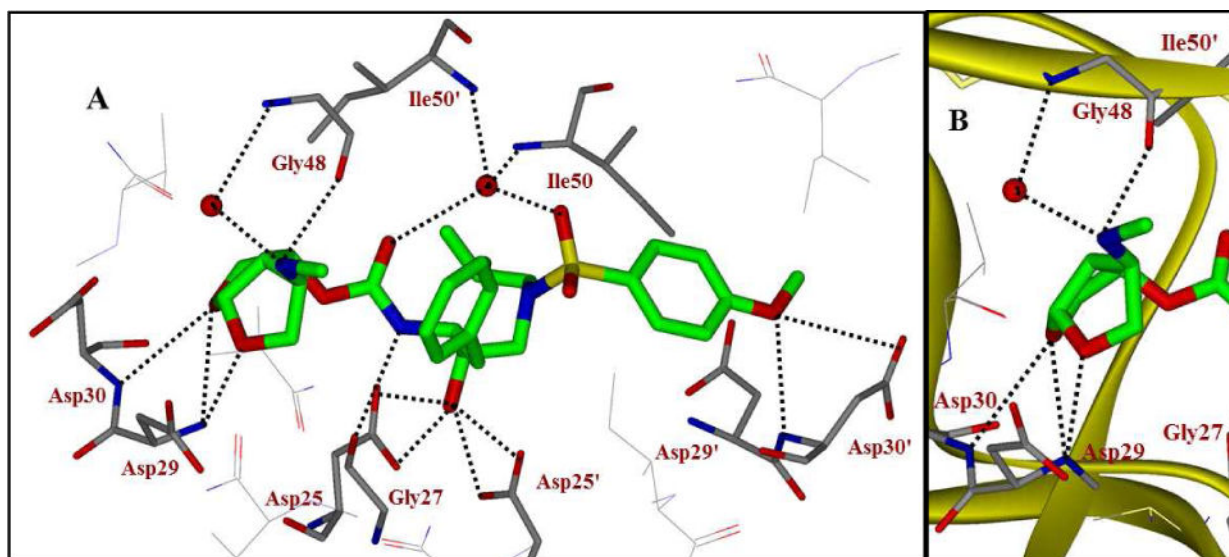
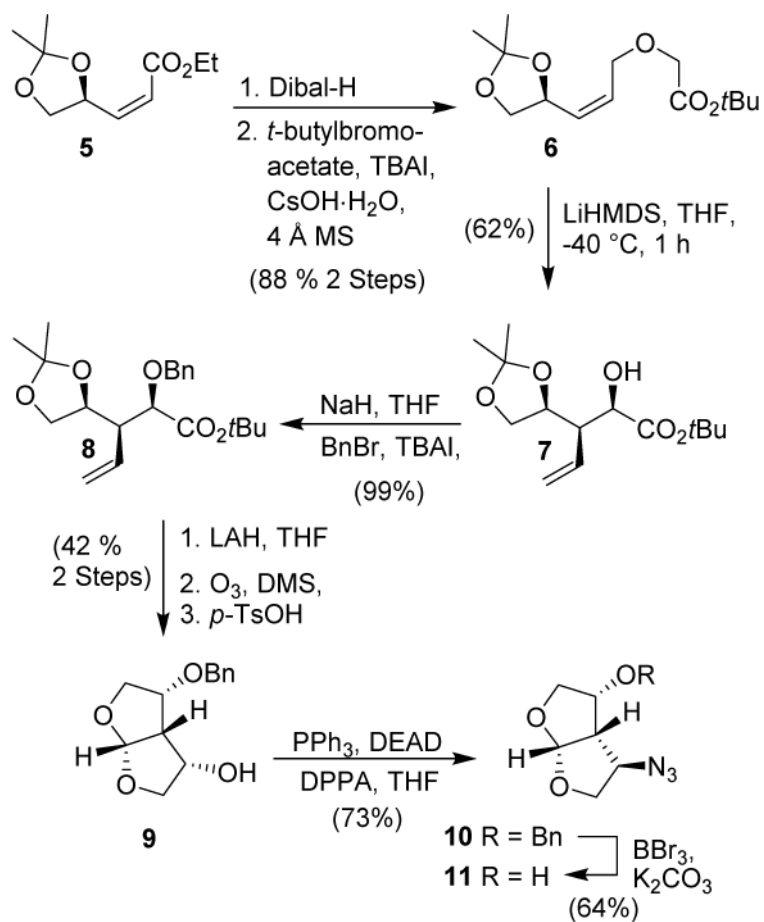
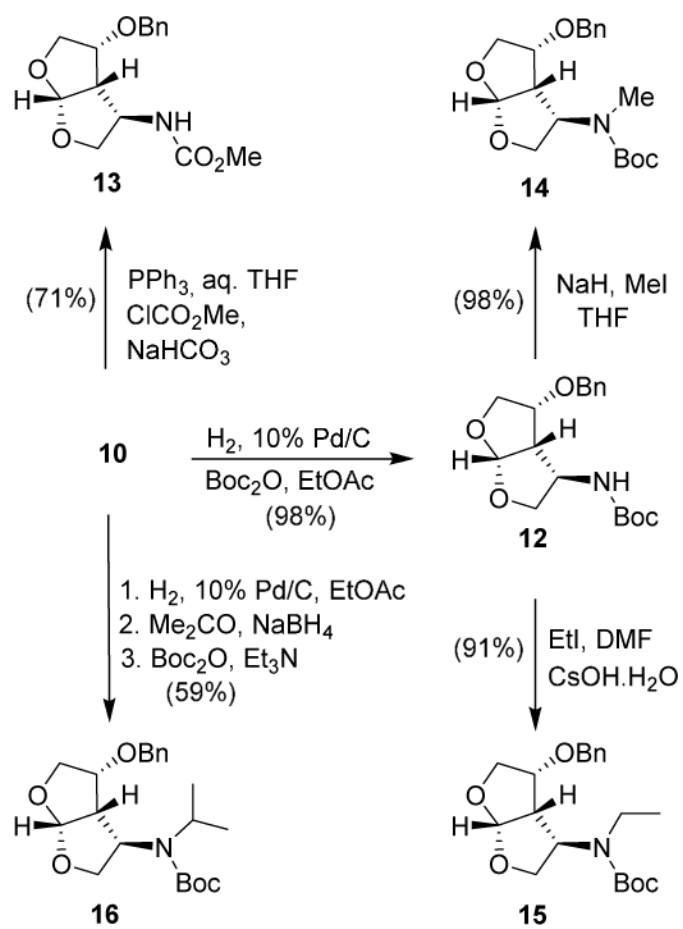


Figure 2.

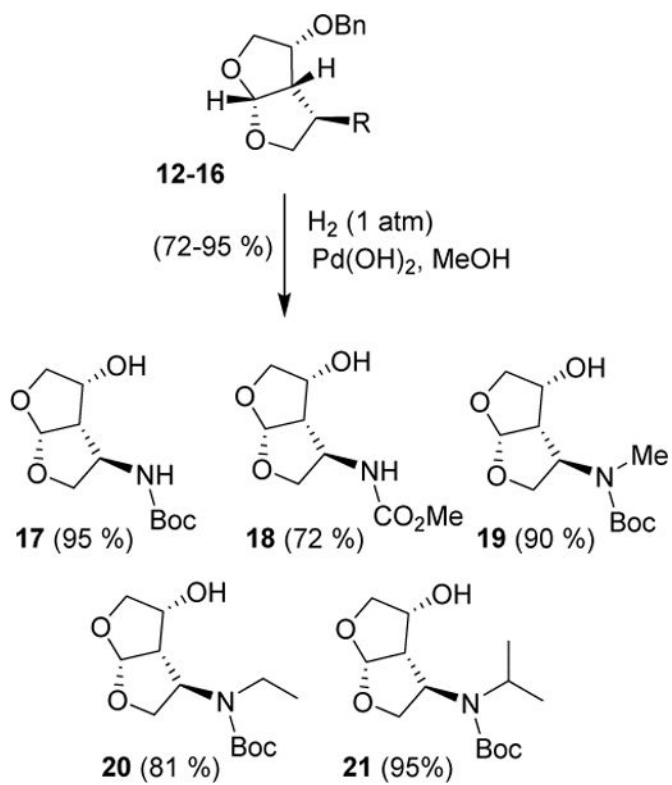
A. X-ray structure of inhibitor **25f**-bound HIV-1 protease (PDB code: 5BRY). Hydrogen bonding interactions are shown as dotted lines. **B.** The main backbone interactions with Gly48 in the flap region and Asp29 and Asp30 in the S2 subsite are shown.



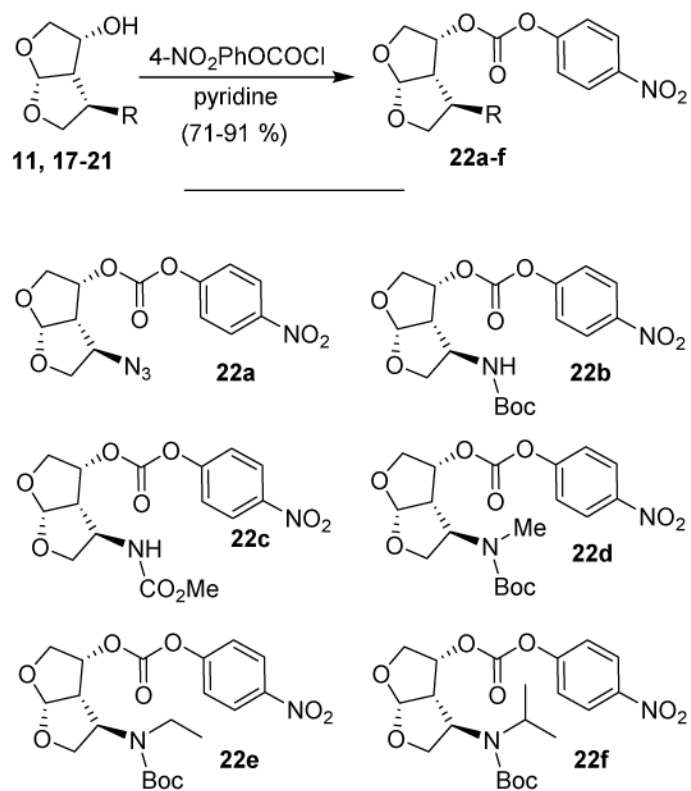
Scheme 1.
Synthesis of azido bis-THF derivatives



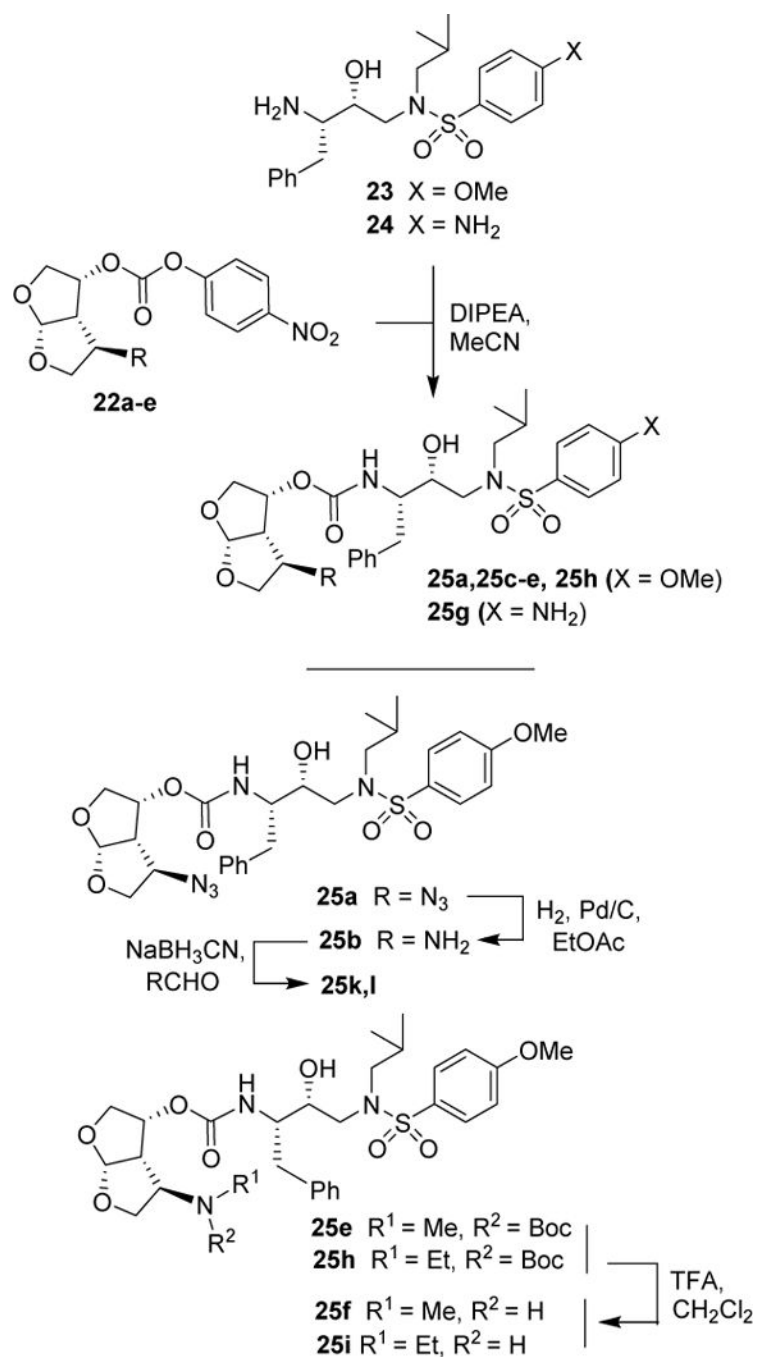
Scheme 2.
Synthesis of various C4-amino bis-THF derivatives



Scheme 3.
Synthesis of various aminoalcohol derivatives



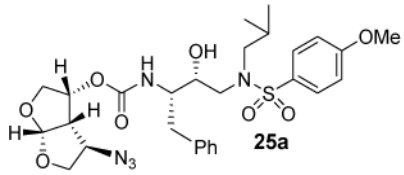
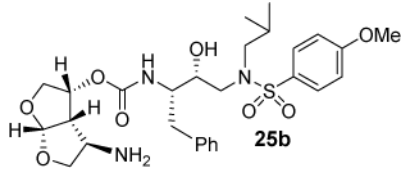
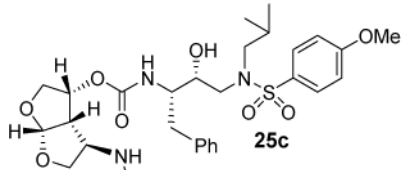
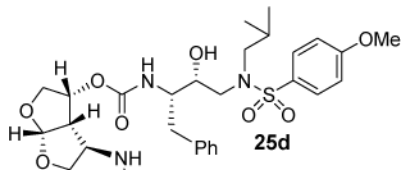
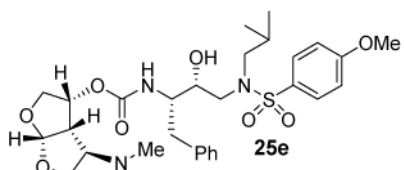
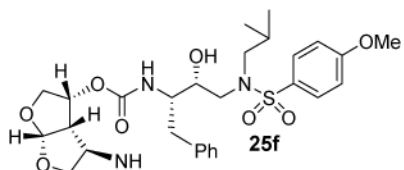
Scheme 4.
Synthesis of active carbonates of bis-THF ligands

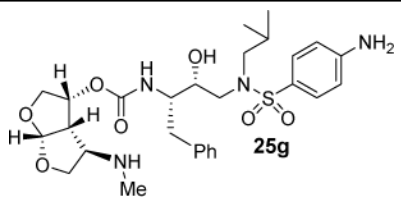
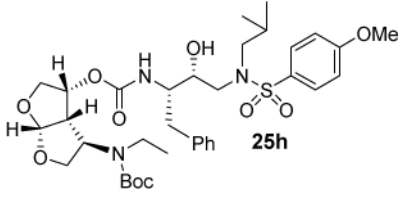
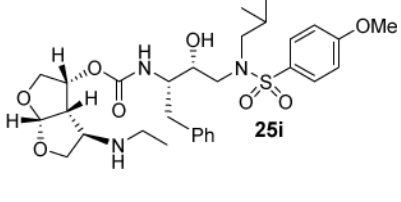
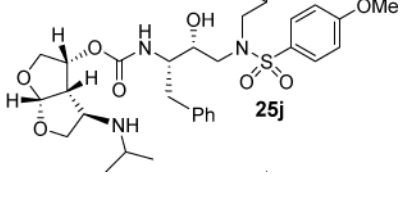
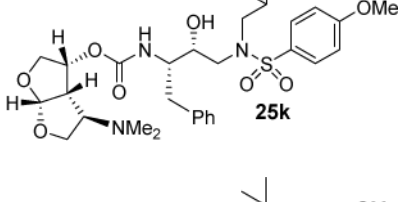
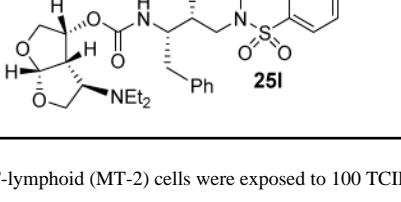


Scheme 5.
 Synthesis of HIV-1 protease inhibitors **25a-1**

Table 1

Enzymatic inhibitory and antiviral activity of inhibitors

Entry	Inhibitor	K_i (nM)	IC_{50} (nM) ^{a,b}
1.	 25a	0.0039	4.4 ± 0.5
2.	 25b	0.53	48 ± 6.5
3.	 25c	0.014	4.4 ± 0.9
4.	 25d	0.024	3.7 ± 0.5
5.	 25e	0.012	37 ± 7.7
6.	 25f	0.0015	35 ± 2.8

Entry	Inhibitor	K_i (nM)	IC_{50} (nM) ^{a,b}
7.	 25g	0.0099	480 ± 31
8.	 25h	0.048	nt
9.	 25i	0.027	22 ± 1.1
10.	 25j	0.0063	0.34 ± 0.2
11.	 25k	0.014	4.4 ± 0.7
12.	 25l	0.014	7.2 ± 0.4

^aHuman T-lymphoid (MT-2) cells were exposed to 100 TCID₅₀ values of HIV-1_{LAI}, and cultured in the presence of each PI, and IC₅₀ values were determined using the MTT assay. Darunavir exhibited K_i = 16 pM, IC₅₀ = 3.0 nM.

^bnt = not tested.

Table 2Antiviral Activity of **25f**, **25i** and **25j** against Multidrug Resistant HIV-1 Variants.

Virus	DRV	<u>EC₅₀ ± SD, (μM) (fold change)^{a,b}</u>		
		Inhibitor 25f	Inhibitor 25i	Inhibitor 25j
HIV-1 _{NL4-3}	0.0026 ± 0.0006	0.029 ± 0.003	0.015 ± 0.003	0.001 ± 0.0033
HIV-1 _{DRV} ^R P10	0.031 ± 0.005 (12)	nd	0.039 ± 0.009 (2.6)	0.021 ± 0.004 (21)
HIV-1 _{DRV} ^R P20	0.097 ± 0.051 (37.3)	0.032 ± 0.003 (1.1)	nd	0.024 ± 0.013 (23)
HIV-1 _{DRV} ^R P51	3.5 ± 1.4 (1346)	nd	0.23 ± 0.08 (15)	0.26 ± 0.12 (260)

^a MT-4 cells (1×10^4) were exposed to 50 TC1D50^S of wild-type HIV-1_{NL4-3}, HIV-1_{DRV} ^RP10, HIV-1_{DRV} ^RP20, or HIV-1_{DRV} ^RP51 and cultured in the presence of various concentrations of each PI, and the IC₅₀ values were determined using the XTT assay. The amino acid substitutions identified in protease of HIV-1_{DRV} ^RP10, HIV-1_{DRV} ^RP20 and HIV-1_{DRV} ^RP51 compared to HIV-1_{NL4-3} include L101/I15V/K20R/L241/V321/M361/M46L/L63P/V82A/L89M; L101/I15V/K20R/L241/V321/M361/M46L/L63P/A71T/V82A/L89M and L101/I15V/K20R/L241/V321/L33F/M36I/M46L/I54M/L63P/K70Q/V82I/I84V/L89M, respectively.

^b All assays were conducted in triplicate, and the data shown represent mean values (± 1 standard deviation) derived from the results of two independent experiments. nd, not determined.